EMPIRICAL AND MODELING STUDIES ON THE PHYSCIAL AND RADIATIVE PROPERTIES OF WINDBLOWN DUST OVER THE COLUMBIA PLATEAU

BY

IRRA T MOHANA SUNDRAM

A dissertation submitted in partial fulfillment of
the requirements for the degree of

DOCTOR OF PHILOSOPHY

WASHINGTON STATE UNIVERSITY
Department of Civil and Environmental Engineering

MAY 2005

To the Faculty of Washington State University:

The members of the Committee appointed to examine the dissertation of IRRA T MOHANA SUNDRAM find it satisfactory and recommend that it be accepted.

_____

Chair

_____

_____

_____

Acknowledgement

I would like to take this opportunity to acknowledge various contributions and support that has enabled the completion of the research reported herein.

The work presented in Chapter 2 resulted from collaborations with Dr. Dave Chandler and Dr. James Kjelgaard, currently at Utah State University and Texas A & M, respectively. Their knowledge and expertise on dust instrumentation were invaluable in the course of the wind tunnel experiments. Mr. Robert Barry of the USDA-ARS had the unenviable task of maintaining the complex operations of the wind tunnel and his unfailing good humor and patience in this regard are very much appreciated.

The work in Chapter 3 was the catalyst for a series of papers focusing on various aspects of simulating regional dust storm events through numerical models. In this regard, I benefited greatly from previous works of Ms. April Miller and Ms. Bennie Lee, former graduate students of Washington State University. I would also like to acknowledge the all the assistance rendered by Dr. Joseph Vaughan and Dr. Susan O'Neill, currently at Washington State University and the Department of Forestry, respectively in modifying and improving the numerical codes.

Chapter 4 research on the sensitivity of the empirically derived dust emission model to various emission factors was initially suggested by Dr. Keith Saxton, formerly of the USDA-ARS during my preliminary doctoral examination in 2003. His assistance in

motivating the direction of this work is greatly appreciated. I would also like to acknowledge Dr. Brenton Sharratt of the USDA-ARS, for the myriad of ideas that shaped this work.

The work presented in Chapter 5 represents the crystallization of an idea initially prompted from research that I had the good fortune to participate in during a summer internship at NASA Goddard for Space Studies (GISS) in 2002. During that period, I benefited greatly from the tutelage of Dr. James Hansen and Dr. Ron Miller of GISS and the opportunity to work with the general circulation models at NASA. In the subsequent phases of this research, I also benefited from conversations with Dr. Nels Laulainen of the Pacific Northwest National Laboratory and Dr. Joseph Vaughan of Washington State University.

The greatest motivation for my research however, has always been the wonderful colleagues that I have been extremely fortunate to collaborate and socialize with during my graduate career. My doctoral committee: Professors Candis Claiborn, Brian Lamb, George Mount and Keith Saxton, have always encouraged me in all my academic endeavors by providing support, motivation and constructive criticisms. Their unwavering belief in my abilities served to fuel my perseverance and determination to succeed in graduate school. My incomparable colleagues, Dr. Laura Wendling, Ms. Jennifer Shaltanis, Ms. Maya Place, Mr. Ranil Dhammapala and Mr. Jorge Jiminez, have always been my staunchest allies and best friends. Last but not least, Dr. Artashes Khachatryan, whose steadfast love and unstinting support is a continuing source of inspiration for me.

EMPIRICAL AND MODELING STUDIES ON THE PHYSCIAL AND RADIATIVE PROPERTIES OF WINDBLOWN DUST OVER THE COLUMBIA PLATEAU

Abstract

By Irra T Mohana Sundram, Ph.D.

Washington State University

May 2005

Chair: Candis S. Claiborn

The research presented here is part of a multidisciplinary wind erosion program, Columbia Plateau PM_{10} Project (CP^3), aimed at evaluating the effects of windblown dust on air quality through intensive field campaigns and application of numerical modeling of emission, transport and dispersion of windblown dust. In the first section, wind tunnel experiments were conducted to evaluate the collection efficiencies of several dust samplers commonly deployed in field campaigns. In dust storm conditions (wind speeds of 7 to 15 m s^{-1}, dust mass loading of 0.42 to 1.11 g s^{-1}), collection efficiencies ranged from < 40 to 100 %. Next, the emission, transport and dispersion of PM_{10} (particulate matter with an aerodynamic diameter less than 10 μm) were numerically simulated for six regional dust storm events. The modeling system included the prognostic meteorological model, Mesoscale Metorological Model Version 5 (MM5), the CALMET/CALGRID Eulerian modeling pair and a dust emission module (EMIT-PM). Improved parameterizations in EMIT-PM resulted in good agreement between observed and predicted 24-hour average

PM_{10} concentrations (ratios between 0.5 to 6.0). The model performance improved with increasing magnitude of the dust storm. Sensitivity tests of the modeling system were also conducted on PM_{10} emissions and concentrations by varying emission variables for the different land use categories and soil classes in eastern Washington. Predicted emissions were significantly influenced by soil crusting, random soil roughness and vegetative surface. A 40 % reduction in the coverage of dry fallow lands resulted in a factor of 2 to 3 reduction in downwind PM_{10} concentrations compared to a 7 to 9 % reduction when surface cover was increased by 50 %. Finally, aerosol optical depths (AOD) were predicted for two dust storm events and values ranged from 0.3 to 0.7, comparable to values in published literature. Sensitivity analyses indicated the magnitude of error for the modeled AOD values ranged from ± 10 to ± 30 %. Aerosol optical depths may prove to be much more useful for model validation than point concentrations in receptor areas, and they also provide information on the role of mineral dusts in regional and global radiation balances.

TABLE OF CONTENTS

LIST OF TABLES

LIST OF FIGURES

CHAPTER 5: Modeling aerosol optical depths during episodes of windblown dust from semiarid agricultural regions

ATTRIBUTION

This dissertation comprises six chapters. In Chapter 1, the objectives and motivation for the research presented in each chapter are established. Chapters 2, 3, 4 and 5 consist of individual manuscripts detailing specific aspects of the overall research, formatted for submission to peer reviewed scientific journals. Chapter 6 is the concluding chapter and also presents recommendations for future applications of the research presented in this dissertation. For each chapter, I was the primarily author and had primary responsibilities for the analyses. Others made contributions as indicated below.

Chapter 2: Evaluating the Performance of Dust Samplers in a Wind Tunnel Under High Wind Speed Conditions

Wind tunnel operations and data collection were initialized and managed by Irra Sundram, Dave Chandler and James Kjelgaard. Keith Saxton provided technical advice on the logistics involved in wind tunnel operations and on the dust sampling instrumentations. Candis Claiborn and Brian Lamb provided expertise in interpreting the mass concentrations measured from the various samplers and their relationships in the wind speed regimes tested in the wind tunnel.

Chapter 3: Numerical Modeling of Windblown Dust in the Pacific Northwest with Improved Meteorology and Dust Emission Models

Irra Sundram executed the numerical simulations for all the dust events, from the initial meteorology to the final transport and dispersion model, with technical

assistance from Brian Lamb. Tara Strand was instrumental in providing the necessary meteorological observation files for the six dust events modeled in the study. Candis Claiborn provided technical advise on various aspects of the research. Dave Chandler and Keith Saxton provided the improved dustiness index, an important parameter related to PM_{10} emissions in the model. This chapter has been accepted for publication in the Journal of Geophysical Research.

Chapter 4: Sensitivity Analyses of PM_{10} Windblown Dust Emissions in a Regional Air Quality Model

Irra Sundram modeled the sensitivity analyses with technical assistance and advice from Brian Lamb. Brian Lamb and Candis Claiborn were also instrumental in providing assistance and guidance with respect to feasible agricultural practices that could be implemented by the farming community to reduce wind erosion in eastern Washington. This aspect was an additional focus of the sensitivity analysis study.

Chapter 5: Modeling Aerosol Optical Depths During Episodes of Windblown Dust From Semiarid Agricultural Regions

Irra Sundram implemented the algorithm to compute aerosol optical depths and conducted the subsequent numerical simulations. These predictions were constrained with sensitivity analyses, which were executed by Rachel Sampang, an undergraduate intern working in the Laboratory for Atmospheric Research over the summer of 2004. Brian Lamb and Candis Claiborn provided technical assistance and advise, pertinent in various aspects of this research.

DEDICATION

Dedicated to my mother, Parvathy, and my grandmother, Aminiamal

for a lifetime of unconditional love and treasured memories

CHAPTER 1: INTRODUCTION

The Columbia Plateau in the Pacific Northwest is a prime example of an arid to semi-arid environment, where the practice of dry land agriculture has rendered much of the region susceptible to wind erosion during the spring and fall months. The multi-disciplinary, multi-agency Columbia Plateau PM_{10} Project (CP^3), supported by the US EPA, the USDA and the Washington State Department of Ecology, was designed to evaluate the magnitude of degradation of soil resource and air quality, specifically from the emission and suspension of particulate matter designated as PM_{10} (particulates with aerodynamic diameters < 10 μm) [*Saxton* 1995]. Achieving these objectives required the incorporation of field campaigns utilizing dust sampling instrumentation capable of measuring horizontal dust fluxes and vertical PM_{10} concentrations and fluxes with an empirical emissions model which could be used in conjunction with other numerical models to predict the transport and dispersion of PM_{10} in the region [*Saxton et al.*, 2000].

Field campaigns on the Columbia Plateau are carried out annually from late spring through the fall seasons. On suitable field sites, usually consisting of fallow land, passive dust samplers such as the Big Spring Number Eight (BSNE) and active samplers capable of measuring PM_{10} concentrations such as the Graseby-Anderson High Volume sampler and the real-time monitors, Tapered Element Oscillating Microbalance (TEOM) and the Air Quality 10 (AQ-10) nephelometers are routinely employed to make measurements in dusty conditions with wind speeds exceeding 7 m s^{-1}. In these conditions, knowledge of collection efficiencies of the samplers is critical to determine the overall confidence in data collected

from these field measurements. Our efforts to ascertain the collection efficiencies of several commonly operated dust samplers in conditions comparable to a dust storm event motivated the research presented in Chapter 2, which is formatted in style of the journal, *Atmospheric Environment.*

The early development of the PM_{10} emissions model based on the landuse categories and soil type for the Columbia Plateau was reflected in the original empirical model, EMIT. This model was employed in conjunction with observed and predicted meteorological data to predict PM_{10} emissions and subsequent transport and dispersion during dust storm events, characterized by elevated PM_{10} concentrations (exceeding 120 $\mu g\ m^{-3}$) in downwind urban locations [*Claiborn et al.*, 1998, *Lee* 1998]. Use of EMIT required invoking a dust calibration constant. However, we were interested in developing a standard approach to predicting the meteorology utilizing the prognostic model, MM5 (version 3) and the diagnostic model, CALMET. In addition, we were also interested in utilizing the revised PM_{10} emission factors (i.e. soil dustiness index in EMIT-PM) developed by *Chandler et al.*[2002] and predicting PM_{10} emissions and concentrations without having to invoke a dust calibration constant to improve predictions, hence, reflecting our improved understanding of the physical processes that influence wind erosion on the plateau. This was the motivation for the research presented in Chapter 3 and the manuscript was formatted in the style of the *Journal of Geophysical Research*.

An important aspect of an empirical model developed from statistical relationships is the overall robustness of the model with respect to perturbations applied to the individual variables. EMIT-PM is a semi-empirical model, developed from statistical relationships between variables influencing dust emission from agricultural fields. These variables, such

as threshold wind speeds for PM_{10} emissions, soil crusting, surface and random roughness and erodibility potentials were developed by *Saxton et al.* [2000] through numerous field measurements, wind tunnel tests and laboratory analyses. However, we were interested to evaluate the overall sensitivity of EMIT-PM to the uncertainties inherent in each PM_{10} emission parameter, in terms of the predicted PM_{10} mass from the spatially inhomogeneous terrain. A related focus of this research was the effect of potential changes in agricultural practices on ambient PM_{10} concentrations. These two sections are presented in Chapter 4 in the form of a manuscript formatted for the journal, *Atmospheric Environment*.

Aerosol climatology, which describes aerosol-climate interactions usually represented by atmospheric turbidity, has important scientific and policy implications for global climate change, yet presents the greatest source of uncertainty in estimates of climate forcing [*Power* 2001]. On a global scale, general circulation models estimate turbidity from mineral aerosols using gridded models with horizontal spatial resolutions in the range of 400 to 500 km [*Chin et al.*, 2002, *Ginoux et al.*, 2001]. However, these low-resolution models lead to large uncertainties in the assessment of radiative forcing. These uncertainties can be reduced by the development and incorporation of high-resolution regional scale models [*Sokolik and Toon*, 1997]. Our overall motivation was to enhance our capability to predict regional PM_{10} emission, transport and dispersion by incorporating algorithms to predict temporally resolved turbidities of individual dust storm events in eastern Washington, which could complement turbidity predictions of mineral aerosol from global circulation models. This facet of the research is presented as a manuscript formatted for the *Journal of Geophysical Research* in Chapter 5.

REFERENCES

Chandler, D. G., K. E. Saxton, J. Kjelgaard, and A. J. Busacca, A technique to measure fine-dust emission potentials during wind erosion, *J. Soil Sci. Soc. Am.*, *66*, 1127 – 1133, 2002.

Chin, M., P. Ginoux, S. Kinne, O. Torres, B. N. Holben, B. N. Duncan, R. V. Martin, J. A. Logan, A. Higurashi, and T. Nakajima, Tropospheric aerosol optical thickness from the GOCART model and comparisons with satellite and sun photometer measurements, *J. Atmos. Sci.*, *59*, 461 – 483, 2002.

Claiborn, C., B. Lamb, A. Miller, J. Beseda, B. Clode, J. Vaughan, L. Kang, and C. Newvine, Regional measurements and modeling of windblown agricultural dust: The Columbia Plateau PM_{10} program, *J. Geophys. Res.*, *103*, 19753 – 19767, 1998.

Ginoux, P., M. Chin, I. Tegen, J. M. Prospero, B. Holben, O. Dubovik, and S.-J. Lin, Sources and distributions of dust aerosols simulated with the GOCART model, *J. Geophys. Res.*, *106*, 20255 – 20273, 2001

Lee, B.-H., Regional air quality modeling of PM_{10} due to windblown dust on the Columbia Plateau, M.S. thesis, Washington State University, Pullman, 1998.

Power, H.C., Estimating atmospheric turbidity from climate data, *Atmos. Environ.*, *35*, 125 – 134.

Saxton, K. E., Wind erosion and its impact on off-site air quality in the Columbia Plateau – An integrated research plan, *Transac. of the ASAE*, *38*, 1031 – 1038, 1995.

Saxton, K. E., D. Chandler, L. Stetler, B. Lamb, C. Claiborn, and B.-H. Lee, Wind erosion and fugitive dust fluxes on agricultural lands in the Pacific Northwest, *Transac. of the ASAE*, *43*, 623 - 630, 2000.

Sokolik, I.N., and O.B. Toon, Regional direct radiative forcing by the airborne mineral aerosols, *J. Aerosol Sci.*, *28 (Suppl. 1)*, S655 – S656, 1997.

Chapter 2

Evaluating the Performance of Dust Samplers in a Wind Tunnel Under High Wind Speed Conditions

Evaluating the Performance of Dust Samplers in a Wind Tunnel Under High Wind Speed Conditions

Irra Sundram, Candis Claiborn, Brian Lamb
Laboratory for Atmospheric Research,
Department of Civil and Environmental Engineering,
Washington State University,
Pullman, 99164, Washington

Dave Chandler,
Department of Plants, Soils and Biometeorology,
Utah State University,
Logan, 84322, Utah

James Kjelgaard
Environmental Physics
Soil and Crop Sciences
Texas A & M University
2474 TAMU
College Station, 77843-2474, Texas

Keith Saxton
USDA – ARS
L.J. Smith Hall - Washington State University
Pullman, 99165, Washington

* Corresponding author.

E-mail address: irra_t-mohanasu@wsu.edu

Tel.: + 1-509-335-6248

Fax.: + 1-509-335-7632

ABSTRACT

Intensive wind erosion field campaigns in the Columbia Plateau of eastern Washington involve deploying commercially available samplers to make representative measurements of dust concentrations in ambient and elevated dust loading conditions. A series of wind tunnel experiments was carried out to evaluate the performance of several dust samplers in conditions relevant to a dust storm event. The Shrouded Probe (S.P.), Air Quality 10 (AQ-10) and Big Spring Number Eight (BSNE) samplers were evaluated against a High Volume (H.V.) sampler, which was modified for isokinetic sampling in wind speeds ranging from 7 to 15 m s^{-1}. Dust mass loading into the wind tunnel ranged from 0.42 to 1.11 g s^{-1}. In terms of mass concentration for 5 and 30 μm material, the collection efficiency of the S.P., without incorporating losses from wall deposition, was < 40 %. Utilizing sieved and dried field soil (< 125 μm), the BSNE had sampling efficiencies of 60 to 100 %. The Tapered Element Oscillating Microbalance (TEOM) measured 1 to 7 % PM_{10} fraction in the field soil as wind speeds were increased from 8 to 15 m s^{-1}. The AQ-10 responses (in mV) had good agreement with the H.V. concentrations (R^2 = 82 %) at wind speeds < 12 m s^{-1} and regression analyses indicated a non-linear relationship between the AQ-10 responses and H.V. mass concentrations.

Keywords: Wind erosion, dust samplers, isokinetic, wind tunnel, collection efficiency

2.1 INTRODUCTION

The accurate measurements of suspended dust concentrations and size distributions are dependent on sampling and collection efficiencies of the aerosol sampler. Most dust samplers are designed to allow particles to enter through an orifice and be trapped onto an exposed filter. To expedite this process, some of these samplers have active pumps drawing in measured amounts of airflow. However, most sampling inlets perturb the airflow trajectory and as a result may have sampling efficiencies above or below a 100 %, due to frictional losses, particle motion and intensity of airflow acceleration near the sampling inlet (Goossens and Offer, 2000). Therefore, in order to make accurate interpretations of field measurements from any sampler, it is necessary to understand the collection efficiency in relevant conditions. These relevant conditions, which either mimic ambient or dusty conditions, can be achieved through laboratory wind tunnel experiments and / or field applications of the wind tunnel (Pietersma et al., 1996).

Correct experimental procedure to understand the behavior of a dust sampler in a wind tunnel requires quantitative comparisons of mass concentrations or horizontal flux measurements with an isokinetic sampler. An isokinetic sampler is the ideal sampler, as theoretically, it does not cause a distortion in the airflow at the sampling orifice. Therefore an isokinetic inlet should allow a 100 % sampling efficiency, though this is rarely achieved due to particle rebound and transmission losses (Goossens and Offer, 2000). Thus, it is important to estimate the absolute efficiency of a sampler as a function of wind speed and in high dust loading conditions prior to field deployment in areas prone to dust storm events.

The study is part of the wind erosion program initiated in 1993 for the Columbia Plateau (Washington) region. This comprehensive program comprising intensive field

campaigns and numerical based modeling was developed in response to windblown dust episodes from the agricultural regions on the plateau causing violations of the National Ambient Air Quality Standards (NAAQS) for PM_{10} concentrations in several downwind urban areas (Claiborn et al., 1998). The main intent of this study was to assess the performance of several commonly utilized commercially available dust samplers in a wind tunnel under conditions comparable to a dust storm event. Since measurements from these samplers in field campaigns provide crucial information on dust emission strengths in source regions, it is important to understand the behavior of these samplers in high wind speed regimes and dust loadings prior to field deployment. The following sections present brief descriptions of the dust samplers, results and discussions of the wind tunnel experiments, followed by a summary and the main conclusions from this study.

2.2 METHODS AND MATERIALS

2.2.1. Description of samplers

The Graseby-Anderson High Volume sampler (IP10 General Motor Works Inc., OH) samples total suspended particulate matter (TSP) by drawing in a measured amount of air ($1.13\ m^3\ min^{-1}$), through an intake hood an onto a filter surface (20.3 x 25.4 cm Quartz Microfibre filter, QM-A, Whatman Int. Ltd.). Airflow is maintained at a constant rate by an electronic probe, which automatically adjusts the speed of the motor to correct for variations in temperature and pressure. For the purpose of this study, isokinetic sampling inlets were designed to replace the original intake configuration on the high volume sampler. Wind speeds in these sampling inlets were designed to agree within ± 3 % of the wind tunnel

velocities, which ranged from 7 to 15 m s^{-1}. A schematic of the high volume sampler configuration in the wind tunnel is presented in Figure 1.

The Air Quality 10 (AQ-10, Environmental Devices Corporation Inc., NY) is a real time nephelometer, which indirectly infers particulate mass concentrations by measuring the intensity of scattered light at 880 nm in a sensing chamber. The AQ-10 has been calibrated with monodisperse, spherical particles of known optical properties. For particles in the size ranges of 1 to 50 μm, the electronic signal responses from the AQ-10 can be directly converted to an equivalent mass concentration. In this study, the sensing unit and corresponding electronic circuitry was mounted in a simple tubular holder with a smooth tunnel shaped inlet, not unlike its field configuration. The entire unit was then clamped onto a metal stand in the wind tunnel (Figure 2).

The shrouded probe is a TSP sampler designed by McFarland et al. (1989) and was employed successfully in wind tunnel experiments by Cain et al. (1998). This sampler is designed to operate at a nominal sampling rate of 0.057 m^3 min^{-1} in velocities of 2 to 14 m s^{-1}. In this study, sample air to the probe was supplied by a vacuum pump (Sogevac SV16 109 81) and a standard flow meter (Key Instruments, FR4000) maintained constant airflow. Prior to placement in the shrouded probe, 47 mm diameter teflon filters (Gelman Laboratory Teflo TM 2.0 μm Pall Co.) were equilibrated for a minimum of 24 hours at 45 % relative humidity.

The Big Spring Number Eight (BSNE) is a TSP sampler designed by Fryrear (1986) to obtain representative samples of suspended soil particles at various heights above the soil surface under varying wind direction regimes. These samplers are easy to construct, robust and can be left unattended in the field. The BSNE is constructed from galvanized metal, stainless steel and 18-mesh screen and when dust-laden air is drawn through the opening, air

speed is reduced and dust settles into a collection pan. In field campaigns, each BSNE usually consists of a series of samplers, from ~0.1 to 1.0 m (Fryrear et al., 1991, Larney et al., 1995). Fryrear (1986) reported a collection efficiency of ~86 % and a retention efficiency of ~ 96 % when tested with eroded material in a wind tunnel.

The Tapered Element Oscillating Microbalance (TEOM) Series 1400 (Rupprecht & Patashnick Co., Inc. NY) is a semi-continuous PM_{10} or $PM_{2.5}$ sampler that operates on the basis of changes in resonant frequency as mass is collected on a 13 mm filter placed at the narrow end of a hollow tapered vibrating glass stack (100 – 150 mm long). Frequency variations are then converted electronically to the reported mass concentrations. In this study, the TEOM was used to measure PM_{10} fraction of the suspended particulate matter in the wind tunnel over a sampling period ranging from 10 to 15 minutes.

In most field campaigns, the AQ-10, BSNE and shrouded probe are utilized to measure TSP although in general, the AQ-10 is more sensitive towards finer particulate matter (< 2.5 μm). In this wind tunnel study, the sampling performances of these instruments are assessed against mass concentrations sampled by the isokinetic high volume sampler, which should be collecting representative samples of dust in the air stream. The TEOM is utilized to measure the fraction of PM_{10} in the suspended dust in the wind tunnel.

2.2.2. Wind tunnel methodology

Soil samples were obtained from a field located near Washtucna, Washington (46° 45'N, 118° 22'W, elevation 500 m), where the USDA/WSU collaborative research team implements field campaigns aimed at characterizing wind blown dust events in the region. These soils, commonly termed Ritzville silt loam (coarse silty mixed mesic *Calcidic*

Haplaxerolls), are loosely structured and have pH values ranging from 6.6 to 8.5 (Horning et al., 1998). The soil was collected in buckets, dried and passed through a 125 μm sieve to exclude clods and coarse debris. The sieved soil had an overall median diameter of 31.5 μm with approximately 90 % (by volume weight) of the soil particles smaller than 81.5 μm. In addition, commercially available 5 and 10 μm red kaolin clay soils (RSG Inc., Sylacauga, Alabama) were also utilized.

The experiments were performed in a USDA-ARS wind tunnel, which has a 7.3 m long, 1.0 m wide and 1.2 m high working section. The basic tunnel is constructed of aluminum sections with a wooden base and a honeycomb/screen section just downwind of the inlet. The purpose of the honeycomb/screen section is to generate and maintain a uniform mean velocity profile within the working section. The variable pitch blades on the fan allow for velocity ranges within the working section from 2 to 20 m s^{-1} (Pietersma et al., 1996).

A continuous stream of the field or commercial soil was added to the air current through an abrader box at the head of the wind tunnel. The soil was fully dispersed and mixed in the wind tunnel via six rigid stainless steel tubes extending from the metering box. The samplers were placed individually downwind in the center of the tunnel (0.5 m) and the inlets were maintained at 0.9 m, above the saltating layer but within the designed boundary layer height of the tunnel and were always oriented into the dust flow. Prior to sampling, wind tunnel velocities were measured for flow consistency with a standard Dwyer Mark II pitot tube installed parallel to the free flow stream in the tunnel. A Campbell Scientific 21x data logger collected wind tunnel velocity measurements and the AQ-10 signals.

2.3 RESULTS AND DISCUSSION

Figure 3 presents the concentrations obtained when 5 μm and 30 μm soil was dispersed in the wind tunnel at a rate of 0.42 ± 0.04 g s^{-1} and 0.80 ± 0.08 g s^{-1}, respectively. In each case, comparative measurements were made with the shrouded probe (S.P.) and the high volume (H.V.) samplers for three wind speeds, 7.8 ± 0.6 m s^{-1}, 11.9 ± 0.1 m s^{-1} and 14.7 ± 0.3 m s^{-1}. For both the 5 μm and 30 μm particles, there was good agreement in terms of the concentration trends as wind speeds were increased even though the S.P. measured only 10 to 35 % of the concentration obtained by the H.V. sampler for both particle sizes. This underestimation could be due to wall deposition in the S.P., which was unaccounted for in the initial experiments.

To investigate this possibility, additional experiments were conducted to take into account wall deposition at wind speeds ranging from 8 to 15 m s^{-1}. Using compressed air, depositions on the wall of the sampler were blown onto the filter and the wall deposition was computed as the difference in sampled mass from a filter that was removed directly after sampling. Results indicated that wall deposition increased with wind speeds and accounted for up to 33 % of the mass collected on the filter at wind speeds > 13 m s^{-1}, which is higher than the 13 % (at a velocity of 14 m $s^{-}1$) obtained by McFarland et al. (1989).

The ability of the BSNE to capture representative samples of field soil at high wind speeds was tested against similar measurements from the H.V. sampler. The field soil was dispersed in the wind tunnel at a rate of 1.11 ± 0.04 g s^{-1}. The results in Table 1 suggest that the BSNE and H.V. samplers are in good agreement in terms of the amount of dust collected at all three wind speeds, with concentration ratios ranging from 0.6 to 1.0. To obtain an estimate of the PM_{10} fraction, the TEOM was also employed under similar mass flow and

wind speed conditions. The PM_{10} fractions in Table 1 were computed with respect to H.V. concentrations and indicate that the amount of fine suspended material increases at higher wind speeds. In general, soils in eastern Washington have approximately a 4 % PM_{10} fraction (Saxton, 1995). However, at higher wind speeds (> 12 m s^{-1}), the larger particles could have been abraded, thus increasing the fraction of fine particles available for collection in the wind tunnel.

The AQ-10 and H.V. samplers were deployed in the wind tunnel at six different wind speeds; 6.78 ± 0.45 m s^{-1}, 8.66 ± 0.43 m s^{-1}, 10.65 ± 0.53 m s^{-1}, 11.82 ± 0.54 m s^{-1}, 12.92 ± 0.58 m s^{-1} and 15.32 ± 0.31 m s^{-1}. The general concentration trends from both these samplers, as presented in Figure 4 were well matched at wind speeds < 12 m s^{-1}. At wind speeds > 12 m s^{-1}, response from the AQ-10 was gradually monotonic, which could be due to the increase of fine particles at higher wind speeds resulting in multiple scattering within the sensing chamber and dust deposition on the sensors. The relationship between the AQ-10 and H.V. sampler was also statistically analyzed in Figure 5. Regression statistics yielded an exponential relationship characterized by a R^2 of 82 %, which suggests that a significant portion of the variation in the AQ-10 responses can be accounted for by the H.V. concentrations. The relationship obtained was;

$$y = 54 \exp(0.7x) \quad (1)$$

where x is mass concentrations (g m^{-3}) and y reflects the electronic signals from the AQ-10 (mV). This relationship appears to indicate that the AQ-10 responses to mass concentrations are best represented by a non-linear relationship, at least for the field soils in this region. However, it would be pertinent to conduct similar experiments at higher (> 15 m s^{-1}) and lower (< 5 m s^{-1}) wind speeds to further investigate the nature of this relationship.

In general, besides sampling and collection efficiencies, sampling line losses, intake efficiencies and flow rate consistencies also compromise measurements from air quality samplers. These uncertainties are often expressed as coefficients of variations (%), which encompass both systematic and random errors for each measurement. Systematic errors are mostly associated with the detection limits of the equipment; ±1.5 % for the Met One reference anemometer, ± 0.02 % for the Campbell Scientific 21x data logger, ± 10.0 % for the optical particle sensor and ± 10.0 % associated with the pumping efficiency of the H.V. sampler. Based on the results of this study, the potential errors associated with the S.P. is < 35 % and between ± 13 % and ± 22 % for the AQ-10.

2.4 SUMMARY AND CONCLUSIONS

Wind tunnel experiments were conducted to evaluate the sampling efficiencies of three dust samplers, the Shrouded Probe (S.P.), Air Quality 10 (AQ-10) and the Big Spring Number Eight (BSNE) at high wind speeds and dust loading conditions. These samplers were evaluated against a Graseby-Anderson High Volume sampler (H.V.), which was modified to have isokinetic inlets at different wind speeds in the wind tunnel. The S.P. sampler had an overall sampling efficiency of < 40 % for 5 and 30 μm for commercially available soil at wind speeds ranging from 8 to 15 m s^{-1}, without taking into consideration losses due to wall deposition. Utilizing sieved and dried field soil at similar wind speeds with the BSNE samplers yielded collection efficiencies ranging from 60 to 100 %.

The Tapered Element Oscillating Microbalance (TEOM), which measures the PM_{10} fraction of suspended dust, was also evaluated with the H.V. sampler. The PM_{10} fraction of the suspended dust in the wind tunnel appeared to increase from 1 to 7 % as wind speeds

increased from 8 to 15 m s^{-1}. The AQ-10 responses were in good qualitative agreement when compared with measurements from the H.V. concentrations for wind speeds ranging from 7 to 12 m s^{-1}, but did not present a linear relationship with mass concentrations.

Based on the results of this study, the BSNE appeared to have the best agreement in terms of mass concentrations with the isokinetic high volume sampler. Besides high sampling efficiencies at wind speeds > 12 m s^{-1}, which is an important consideration during dust storm events, the BSNE has low maintenance requirements in field deployment. Based on the results of their instrumentation calibration study, Goossens and Offer (2000) also recommended the BSNE, even though they only obtained sampling efficiencies (independent of the wind speeds in the wind tunnel) of approximately 40 %. The S.P. performed much poorer when compared to the 82 to 90 % efficiencies obtained by Chandra and McFarland (1995) for 5 to10 μm atomized aerosol particles, in wind speeds of 2 to 14 m s^{-1}. However, the sampling efficiencies of the S.P. would improve by almost 33 % at higher wind speeds if losses from wall deposition were accounted for in the mass concentration computations.

In summary, the experiments detailed in this study present important information on the collection efficiencies of several commonly utilized field dust samplers. Based on the manufacturers specifications, these samplers have >90 % collection efficiencies in ambient to mildly dusty conditions, however, at higher wind speeds and dust loading, the efficiencies of some of these samplers appear to deteriorate significantly (< 50 %). While more extensive research, encompassing higher wind speed regimes and field studies should be considered prior to making conclusive statements on the performances of these samplers in dust storm conditions, these initial findings should be incorporated into interpreting and evaluating field measurements of windblown dust.

ACKNOWLEDGEMENTS

The shrouded probe samplers were kindly provided by Dr. John Rogers and his group at the Health Physics Measurements Group, Los Alamos National Laboratory. We would also like to acknowledge the invaluable assistance of Mr. Robert Barry from the USDA-ARS, Pullman, WA in maintaining and operating the wind tunnel. Contributions from all the CP^3 group members are also acknowledged.

(Tables and Figures follow references)

REFERENCES

Cain, S.A., Ram, M., Woodward, S., 2000. Qualitative and quantitative wind tunnel measurements of the airflow through a shrouded probe airborne aerosol sampling probe. J. Aerosol Sci., 29, 1157 – 1169.

Chandra S., and McFarland, A. R., 1989. Comparison of aerosol sampling with shrouded and unshrouded probe. American Industrial Hygiene Association, 56, 459 – 466.

Claiborn, C., Lamb, B., Miller, A., Beseda, J., Clode, B., Vaughan, J., Kang, L., Newvine, C., 1998. Regional measurements and modeling of windblown agricultural dust: The Columbia Plateau PM_{10} program. J. Geophys. Res., 103, 19753 – 19767.

Fryrear, D.W., Stout, J. E., Hagen, L. J., Vories, E.D., 1991. Wind erosion: Field measurement and analysis. Transactions of the ASAE, 34, 155 – 160.

Goossens, D., and Offer, Z. Y., 2000. Wind tunnel and field calibration of six Aeolian dust samplers. Atmos. Environ., 34, 1043 – 1057.

Larney, F.J., Bullock, M. S., McGinn, S. M., Fryrear, D. W., 1995. Quantifying wind erosion on summer fallow in southern Alberta. J. of Soil and Water Conservation, 50, 91 – 95.

McFarland, A. R., Oritz, C. A., Murray, M. E., DeOtte, R. E. Jr., Somasundaram, S., 1989. A shrouded aerosol sampling probe. Environ. Sci. Technol., 23, 1487 – 1492.

Pietersma, D., Stetler, L. D., Saxton, K. E., 1996. Design and aerodynamics of a portable wind tunnel for soil erosion and fugitive dust research. Transactions of the ASAE, 39, 2075 – 2083.

Saxton, K.E., 1995. Wind erosion and its impact on off-site air quality in the Columbia Plateau – An integrated research plan, Transactions of the ASAE, 38, 1031 – 1038.

Table 1

Big Spring Number Eight (BSNE), High Volume (H.V.) dust concentrations and PM_{10} fractions from the Tapered Element Oscillating Microbalance (TEOM) as a function of wind speeds in a wind tunnel

Wind Speeds ($m\ s^{-1}$)	BSNE concentrations ($g\ m^{-3}$)	BSNE / H.V. concentration ratio	PM_{10} fraction (%)
7.8	0.5 ± 0.1	0.6 ± 0.1	0.8
11.9	0.7 ± 0.1	0.8 ± 0.1	1.4
14.7	0.6 ± 0.1	1.0 ± 0.1	6.7

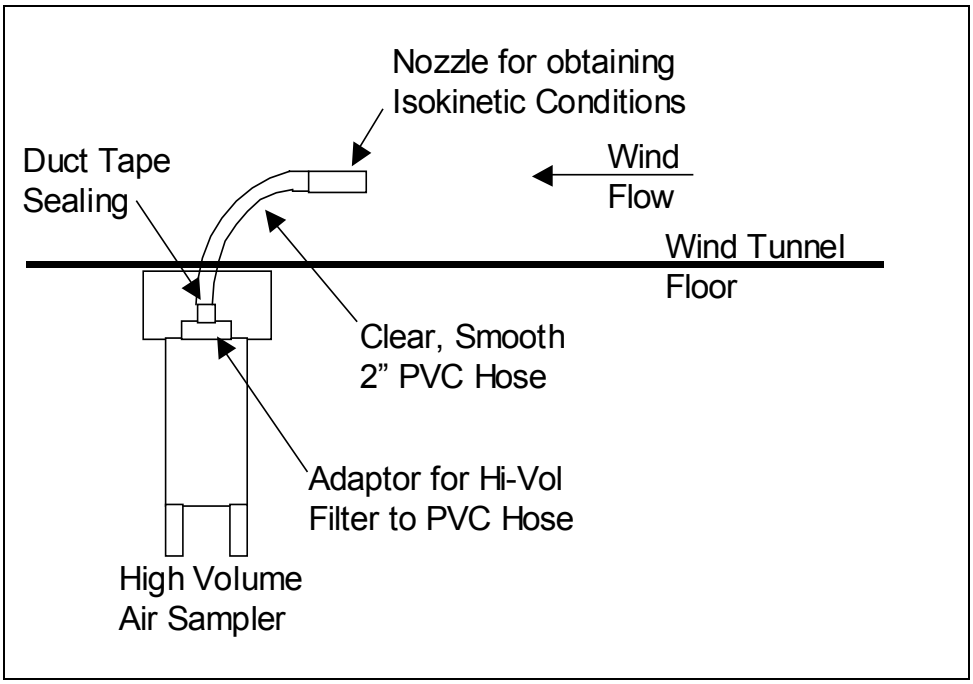

Figure 1. Schematic of the high volume sampler with modified isokinetic sampling inlets in the wind tunnel.

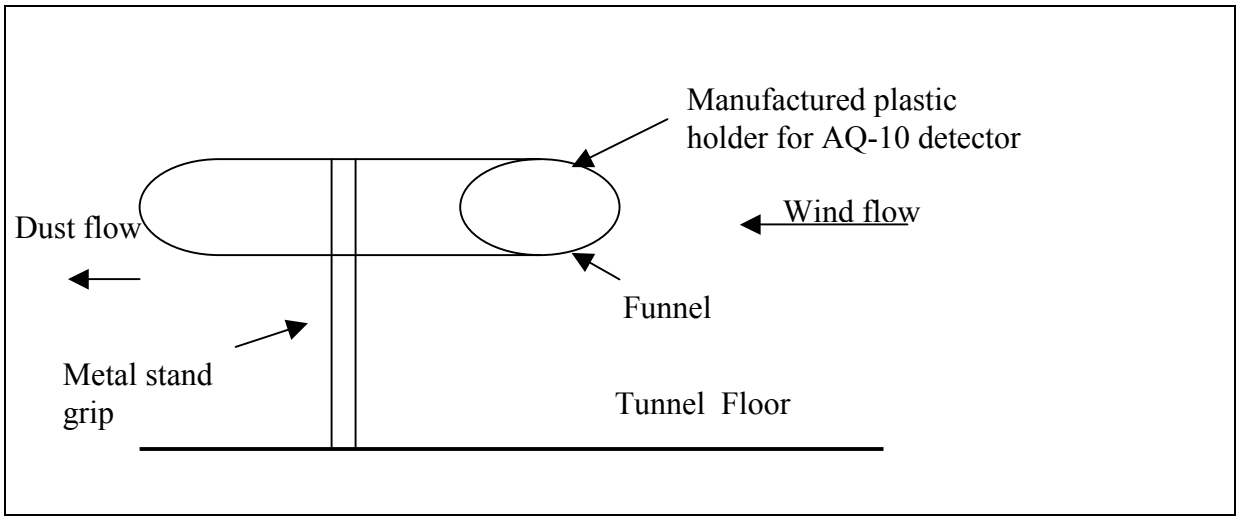

Figure 2. Schematic of the Air Quality 10 (AQ-10) sampler in the wind tunnel

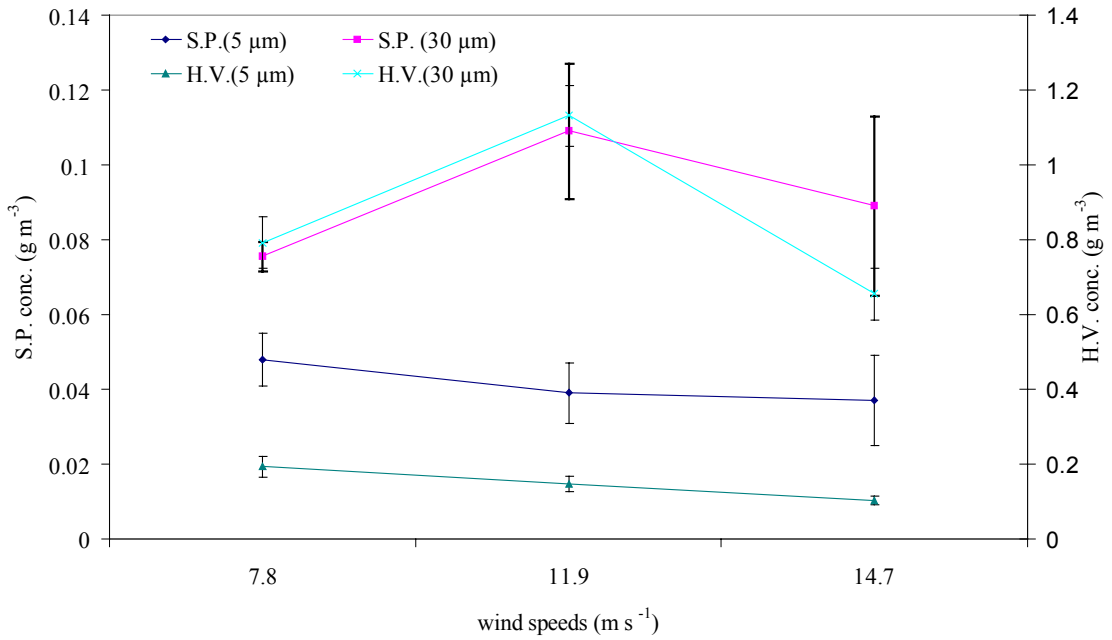

Figure 3. Concentrations of 5 and 30 µm materials measured by a shrouded probe (S.P.) and high volume sampler (H.V.) in a wind tunnel

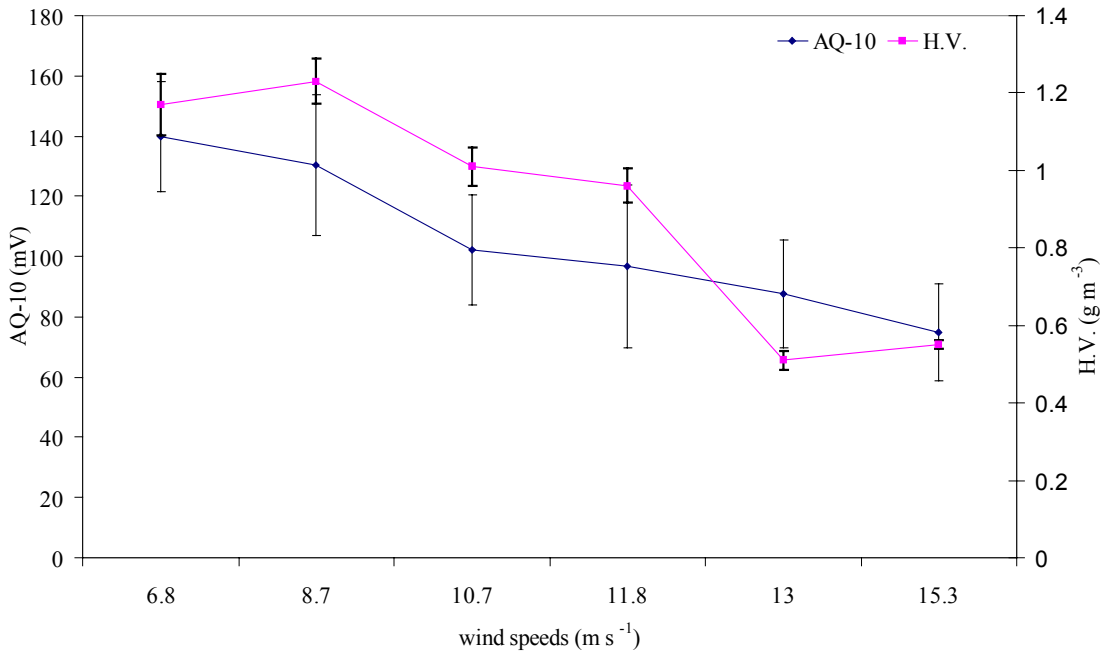

Figure 4. Concentrations of field soil measured by a high volume (H.V.) sampler and corresponding responses from the air quality (AQ-10) sampler in a wind tunnel

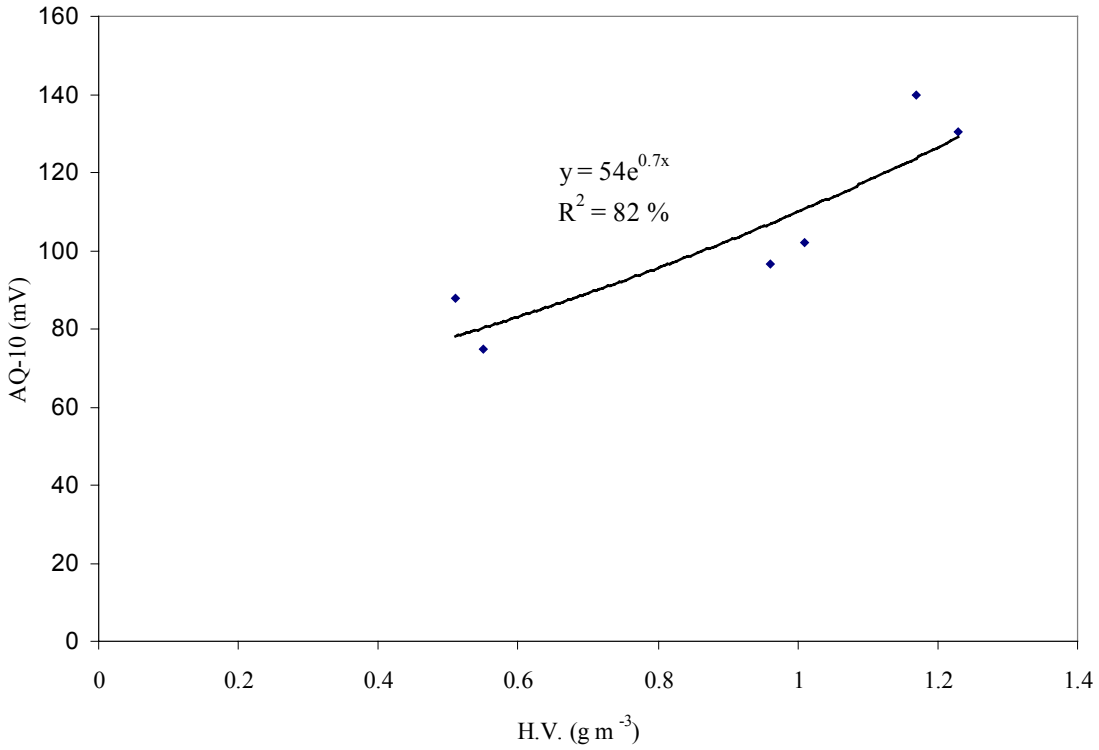

Figure 5. Relationship between concentrations measured by the high volume (H.V.) sampler and responses from the Air Quality 10 (AQ-10) sampler.

Chapter 3

Numerical Modeling of Windblown Dust in the Pacific Northwest with Improved Meteorology and Dust Emission Models

Numerical Modeling of Windblown Dust in the Pacific Northwest with Improved Meteorology and Dust Emission Models

Irra Sundram, Candis Claiborn, Tara Strand, Brian Lamb
Laboratory for Atmospheric Research,
Department of Civil and Environmental Engineering,
Washington State University,
Pullman, 99164, Washington

Dave Chandler,
Department of Plants, Soils and Biometeorology,
Utah State University,
Logan, 84322, Utah

Keith Saxton
USDA – ARS
L.J. Smith Hall - Washington State University
Pullman, 99165, Washington

ABSTRACT

Soil erosion by wind is a serious consequence of dry land agriculture in eastern Washington where the main adverse effects are loss of nutrient-rich soil, reduced visibility during dust storms and degradation of air quality. A multidisciplinary research effort to study windblown dust in central and eastern Washington was initiated under the Columbia Plateau PM_{10} (CP^3) program, which involved measuring wind erosion and windblown dust emissions at sites throughout the region and developing a transport and dispersion model for the area. The modeling system includes the prognostic meteorological model, Mesoscale Metorological Model Version 5 (MM5), coupled with the CALMET/CALGRID Eulerian modeling pair and a new dust emission module (EMIT-PM). Improvements to the modeling system included employing higher spatial resolutions for the meteorological models and improved parameterizations of emission factors in EMIT-PM. Meteorological fields, dust emissions, and the resulting dust concentrations were simulated for six historical regional dust storms: November 23, 1990, October 21, 1991, September 11, 1993, November 3, 1993, August 30, 1996 and September 23 to 25, 1999. For all the simulated events, with the exception of the August 1996 event, ratios of observed to predicted concentrations were favorable, within a range of 0.5 to 6.0, without calibration of the dust emission model. These results showed that the model performed best for large, strong dust storms, but did not simulate smaller storms as well. PM_{10} emissions averaged 22 Gg per 24-hour event, which represents approximately 1 % of the daily dust flux on a global basis. .

3.1 INTRODUCTION

Soil erosion by wind is a serious consequence of dry land agriculture in many parts of the world. This is especially pervasive in the Pacific Northwest where, due to low precipitation rates of 150 to 360 mm / year, dry land farming involves alternate years of cropping and clean tilled fallow land. During the fallow years, the soil is periodically tilled for weed control and this results in loosely structured clods on bare surfaces, which are very susceptible to wind erosion [*Horning et al.*, 1998]. The amount of soil loss from erosion is dependent on the local meteorology and soil morphology, and losses ranging from 0.3 to 30.4 Mg ha $^{-1}$ per erosion event have been reported from monitoring studies in Alberta, Canada [*Larney et al.*, 1995]. An erosion monitoring study in Texas conducted over 18 months, indicated that most erosion events are associated with periods of low humidity (< 30%), low precipitation, no surface cover and daily wind speeds greater than 4 m s $^{-1}$, and similar conditions have also been associated with erosion events in the Pacific Northwest [*Stout* 2001].

The main adverse effects of soil erosion on agriculture in the Pacific Northwest are decline in soil quality due to removal of nutrient rich aggregates, reduced soil productivity and subsequently, reduced crop yield. Windblown dust also leads to air quality and public health issues as finer fractions (< 10 μm) of the entrained dust are transported downwind of the source regions. However, declining visibility is usually of immediate concern during a dust storm episode. For example, visibility in the Korean peninsula decreased from 60 km to 2 km as the hourly PM_{10} concentrations increased from 32 to 600 μg m $^{-3}$ during the Chinese Yellow Sand event in 2000 [*Kim et al.*, 2001]. In the Pacific Northwest, poor visibility during a dust storm event in 1999 resulted in a fifty car pile-up and seven deaths on Interstate

84 near Hermiston, Oregon. These adverse effects coupled with violations of the National Ambient Air Quality Standards for PM_{10} in several urban areas in eastern Washington motivated the formation and long-term support of the Columbia Plateau PM_{10} Program (http://pnw-winderosion.wsu.edu).

In recent years, there has been considerable debate on the climate forcing potential of atmospheric dust, with current global emissions estimated to range between 1000 to 5000 Tg yr^{-1} [*Xuan and Sokolik*, 2002, *Ginoux et al.*, 2001, *Houser and Nickling*, 2001]. Since 30 to 50 % of the dust load is predicted to originate from soil disturbed by human activities, determination of this forcing potential should consider climate-anthropogenic activities feedback cycles [*Tegen and Fung*, 1995]. However, sparse information on the microphysical, chemical and optical properties of atmospheric dust contribute toward the unresolved and poorly understood issue of the influence of atmospheric dust on local climatology and on global and regional radiative budgets [*Tegen* 2003, *Yu et al.*, 2001].

Modeling mobilization of dust from soils is usually described in terms of creep, saltation and resuspension of soil, based on the assumption that vertical dust flux is a function of the surface shear stress [*Houser and Nickling*, 2001, *Tegen and Fung*, 1994, *Fryrear et al.*, 1991]. This assumption is often applied in terms of a power law relationship between the vertical flux of dust and friction velocity: $F = Cu_*^n$, where C is a calibrated, empirical constant. In their global simulation of the atmospheric dust cycle, *Tegen and Fung* [1994] adjusted C to obtain agreement between predicted and estimated source strengths; the range of C was between 0.4 and 1.2 $\mu g\ s^2\ m^{-5}$ in the relationship $F = C\ (u-u_t)^n$ where u_t is a threshold wind speed that must be exceeded in order to produce windblown dust. *Ginoux et al.* [2001] improved dust source characterizations in the GOCART model and were able to

reproduce seasonal variations of global surface concentrations using a C value of 1 $\mu g\ s^2\ m^{-5}$.

On a regional scale, mobilization of soil from eroding surfaces has been further parameterized in terms of physical soil properties such as mechanical stability of clods, aggregates, crust, surface cover and roughness conditions [*Draxler et al.,* 2001, *Horning et al.*, 1998]. To develop their dust production model (DPM), *Alfaro and Gomes* [2001] combined empirical based models describing saltation and sandblasting and successfully validated the DPM with field measurements for PM_{20} emissions from various soil types in Spain and Niger [*Gomes et al.*, 2003]. *Draxler et al.* [2001] parameterized vertical mass flux for PM_{10} for sandy desert soil using friction velocity, threshold friction velocity and a parameter defining surface soil textures. In eastern Washington, a dust model (EMIT) based on abrasion and suspension processes was developed for PM_{10} emissions through independent experiments characterizing the effect of emission variables (e.g. roughness elements, surface crusting) on total emissions for specific soil types and farming practices. Statistical analyses were then employed to develop relationships between horizontal soil flux and PM_{10} emissions [*Saxton et al.,* 2000, *Horning et al.*, 1998, *Saxton 1995*].

For validation, *Claiborn et al.* [1998] employed EMIT with the CALMET/CALGRID models to simulate two dust storms in eastern Washington and found that C values of 9.6 x 10^{-3} and 1.5 x 10^{-3} $g\ s^3\ m^6$ were required to achieve ratios of observed to predicted PM_{10} concentrations of 0.5 to 3.6. Variations in C in that study reflected changes in soil parameters, especially moisture content, over the fall season. Based on the recommendations from *Claiborn et al.* [1998], efforts to improve the dust emission algorithm were carried out by *Saxton et al.* [2000]. This resulted in a modified emissions model (EMIT-PM), developed

specifically for the Pacific Northwest from extensive soil sampling, portable wind tunnel and intensive field measurements. *Lee* [1998] utilized the revised code to model five dust storm events, which occurred in the Pacific Northwest, but C still required calibration to match predictions to available observations. In the study by *Lee* [1998], the values for C accounted for the overall effects of remaining uncertainties in the emissions model and exhibited large fluctuations for the different events. Subsequently, *Chandler et al*. [2002] incorporated better estimates of the suspendable soil fraction (PM_{10}), described by the soil dustiness index in the emission algorithm, in a revised version of the EMIT-PM.

The intent of this study was to evaluate the improvements in EMIT-PM as part of a high-resolution regional windblown dust model to predict PM_{10} emissions, transport and dispersion for large regional dust storms in the Pacific Northwest. This modeling effort has important regulatory implications since several populated areas in eastern Washington (e.g. Spokane) have been designated as 'non-attainment' areas for PM_{10} concentrations in the past and therefore, appropriate erosion mitigation strategies are required to control urban air quality impact from agricultural wind erosion [*Saxton* 1995]. Development of this regional modeling system also provides a foundation for investigation of the effectiveness of wind erosion control strategies (e.g. increase in vegetative surface cover) in reducing PM_{10} concentrations in downwind populated areas and the impact of intense regional dust storms upon aerosol optical depth and in turn, global climate change.

Utilization of the revised EMIT-PM in conjunction with MM5, CALMET and CALGRID in this study provided an opportunity to identify dust sources and quantify PM_{10} emissions from agricultural regions and predict hourly variations of PM_{10} concentrations in populated areas during six historical dust storm events in eastern Washington. To test

emission algorithms in EMIT-PM, the calibrated dust constant, C, was not invoked. An overview of the modeling system, including descriptions of the modeling components and the empirically derived emissions parameters, is presented in Section 3.2 and before results from the simulations of six individual case studies are discussed in Section 3.3. Statistical performances of various components of the model are also discussed.

3.2 OVERVIEW OF THE MODELING SYSTEM

3.2.1. The EMIT-PM emissions model

EMIT-PM was developed to determine the fraction of dust emissions contributing from eroding fields that contribute towards PM_{10} regional concentrations. The model is based upon two semi-empirical equations describing horizontal and vertical soil fluxes. The horizontal soil flux as described by *Saxton et al*. [2000] is a function of the available wind energy, soil erodibility, vegetative surface cover, soil surface roughness, soil surface wetting and crusting. Based on extensive wind tunnel and field measurements, these variables can be described empirically in the horizontal soil flux equation:

$$Q_t = W_t * EI * (e^{-0.05 * SC} * e^{-0.52 * K}) * WC \quad (1)$$

Where Q_t is the eroded soil discharge per meter field width per unit time, (g m^{-1} width per hour event) and W_t is the erosive wind energy per unit time (m^3 s^{-3} per hour event). The wind energy term includes a threshold wind speed (U_{te}) required to initiate soil movement on the ground. Based on extensive field characterizations during dust events on the Columbia Plateau, U_{te} was defined as 5.5 m s^{-1} for all events modeled in this study. EI describes the

erodibility potential of unprotected soil (g s^3 m^{-3}) and is calculated from the relative erodibility ratio (ER) obtained from wind tunnel trials for each soil type. SC is the percentage of vegetative soil cover and K describes the random roughness of large soil elements (cm). WC is a non-dimensional index from 0 – 1 describing the degree of wetness and crusting of the soil. Wet, crusted soil has less potential for erosion and is represented by a lower WC value as opposed to higher values associated with dry, disturbed, non-crusted soil [*Saxton et al.*, 2000].

The vertical flux of PM_{10} (g m^{-2} s^{-1}) is described as a function of the horizontal soil flux, soil dustiness, wind velocity and the calibrated non-dimensional dust constant, C (=1 in this study), in the following form:

$$F_d = C * C_v * u_* * Q_t * (D/100) \quad (2)$$

C_v is a units conversion factor, u_* is the friction velocity (m s^{-1}), and D is the soil dustiness index. D was determined by a laboratory procedure utilizing soils sample, which were suspended and abraded in an emission cone prior to measurement of the PM_{10} fraction with a standard measuring instrument [*Chandler et al.*, 2002, *Saxton et al.*, 2000]. D was calculated as the ratio of the mass of suspended PM_{10} collected by the measuring instrument to the mass of suspended soil in the cone. The fraction of suspended PM_{10} as determined by *Chandler et al.* [2002] from suspension and abrasion processes was three to six times higher than previous measurements from *Saxton et al.* [2000] who only considered suspension mechanisms to compute D. Hence, the D values utilized in this study were larger than the

values utilized by *Lee* [1998] and *Claiborn et al.* [1998] and resulted in significantly larger PM_{10} emissions.

Tables 1 and 2 summarize the input variables required for EMIT-PM as functions of landuse categories. SC, K, WC and Zo (aerodynamic roughness, cm) represent regional averages for various landuse categories in the model domain. SC, K and Zo were obtained through wind tunnel trials on 68 field plots and K through visual comparisons of test plots with well documented photographs from other studies [*Saxton et al.*, 2000]. The landuse categories are rangeland (RL), irrigated (IRR), dry crop (DC), dry fallow (DF), and conservation resource program (CRP). In Table 2, values for D reflect improved results from *Chandler et al.* [2002]. D and ER are functions of soil types common to Washington, Oregon and Idaho. L1 is the most erodible soil, L5 is the least erodible soil whereas the D class soils are equal to L1 in terms of erosivity [*Lee* 1998].

3.2.2. The meteorological model MM5, MCIP2, and CALMET

MM5 is a mesoscale meteorological model developed in the early 1970's and currently maintained as a community model by the National Center for Atmospheric Research. MM5 is a prognostic model capable of multiple domain nesting, nonhydrostatic dynamics, four-dimensional data assimilation (FDDA) and a variety of physics options, which allow for representative simulations of the meteorology in the domain of interest [*Dudhia et al.*, 2001]. In this study, MM5 was run in the non-hydrostatic mode to generate the wind fields for all six dust storm events. This application of MM5 for our regional dust modeling is an improvement over previous work by *Claiborn et al*. [1998] and *Lee* [1998] since those studies did not use a consistent meteorological modeling method for each dust

event, and the horizontal grid scale resolution in the parent MM5 simulations were at a coarse scale in most cases.

The horizontal winds from MM5 were utilized as the initial guess field in the diagnostic meteorological model, CALMET. The nested grids in MM5 had horizontal dimensions of 36, 12 and 4 km (Figure 1). The innermost domain (4 km) had 124 x 97 grids (longitude by latitude), which encompassed the state of Washington, northern Oregon and Idaho and southwestern Canada. FDDA, which incorporates analysis nudging, was applied to the 36 and 12 km domains. With this option, user defined relaxation terms are applied to the prognostic equations and this serves to relax the model values towards an analysis obtained for the assimilation period [*Dudhia et al.,* 2001]. The analysis nudging coefficients for wind and temperature fields for the 36 km domain was 2.5×10^{-4} and 1.0×10^{-4} for the 12 km domain. One way nesting was used for interpolation from the 36 to 12 km domain and two way nesting was employed from the 12 km to the 4 km domain. In the vertical dimension, a terrain following coordinate system was utilized with 37 sigma layers.

CALMET was utilized to develop mass consistent, three dimensional wind fields for each event with interpolation of the MM5 winds with available surface wind observations. The innermost 4 km domain from MM5 was reduced to 88 x 76 grids (longitude by latitude), which encompassed an area from 45.425 N to 48.479 N and 121.000 E to 116.105 E (Figure 2). Figure 2 also displays the terrain elevation for this region, where the more mountainous regions corresponding to the Cascade mountain range are to the west and the flatter plains of the Columbia Plateau to the east, with an average elevation of approximately 800 m.

To produce the final wind fields, observational data were introduced through an objective analysis procedure involving an inverse-distance squared interpolation scheme.

This scheme allows for the utilization of observational data in the vicinity of the surface stations and the first step wind fields in regions of sparse or no observational data [*Elbir* 2003]. The meteorological stations are mostly located in eastern Washington and surface data were available from 28 to 75 stations whereas upper air soundings were available from 1 to 4 stations among the six events. The required hourly observational data are wind speed, wind direction, temperature, cloud cover, ceiling cloud height, surface pressure and relative humidity [*Scire et al*., 1999].

The vertical layers were also reduced to 13 layers with the layer faces defined at 20, 36, 70, 110, 145, 215, 290, 400, 506, 656, 1000, 1695 and 3340 m above ground level. These layer heights were chosen to be compatible with the application of the MM5 post-processor; Meteorology-Chemistry Interface Processor (MCIP2). MCIP2 is part of the US EPA's CMAQ modeling system and in this study, was employed to pass MM5 boundary layer terms, including mixed layer height, directly to CALGRID. In this way, the MM5 horizontal winds were interpolated with observations in CALMET, while all other boundary layer terms were obtained directly from MM5 via MCIP.

3.2.3. The transport and dispersion model, CALGRID

CALGRID solves the K-theory form of the atmospheric diffusion equation to obtain hourly averaged values of PM_{10} in each grid cell. In this case, PM_{10} particles are treated as inert tracers. The final transport and diffusion equation solved for each time step in each grid cell can be represented by:

$$\frac{\partial \bar{c}}{\partial t} + \frac{\partial \overline{uc}}{\partial x} + \frac{\partial \overline{vc}}{\partial y} + \frac{\partial \overline{wc}}{\partial z} - \frac{\partial}{\partial x}(Kx\frac{\partial \bar{c}}{\partial x}) - \frac{\partial}{\partial y}(Ky\frac{\partial \bar{c}}{\partial y}) - \frac{\partial}{\partial z}(Kz\frac{\partial \bar{c}}{\partial z}) = R + S + L \quad (3)$$

Where K represents the eddy diffusivity tensor and R represents photochemical processes, which were not utilized in this study, S represents emission sources and L represents losses from deposition processes [*Yamartino et al.*, 1992]. CALGRID employs a higher order chapeau scheme to solve the advection terms. The model employs the Smargorinsky method to compute diffusivities due to distortion or stress in the horizontal wind field. Vertical diffusivities (Kz) are estimated using convective scaling in the daytime boundary layer and local scaling in the nighttime boundary layer [*Scire et al.*, 1989]. The hourly emissions from erodible soil in the target domain (i.e. the S term in the transport and diffusion equation) were provided by EMIT-PM. The horizontal grid system of 88 grids x 76 grids and 13 vertical layers employed in CALMET were maintained for the CALGRID simulations as well. The dry deposition velocity was specified as a constant at 0.1 cm s^{-1}.

3.2.4. Description of PM_{10} episodes and surface observations

Surface measurements of ambient PM_{10} at various receptor sites are available for all six dust storm events and were used to evaluate model predictions. These measurements are gravimetrically determined hourly (TEOM) or averaged 24-hour PM_{10} concentrations, measured by the Spokane and Benton County Air Pollution Control Authorities located in Spokane and Kennewick, WA (see Table 3 and Figure 2). Background concentrations of PM_{10} tend to vary between 30 and 80 μg m^{-3} from rural to urban sites, respectively [*Claiborn et al.,* 1998]. Six dust storm events were simulated and analyzed; November 23, 1990, October 21, 1991, September 11, 1993, November 3, 1993, August 30, 1996, and September

23 to 25, 1999. These events occurred mainly due to strong southwesterly winds associated with low-pressure systems, which resulted in wind speeds exceeding 6.0 m s^{-1} with gusts up to 15 m s^{-1} and violations of the NAAQS standards at one or more of the sampling stations over the source locations and urban areas. *Claiborn et al.* [1998] analyzed a number of dust storms and identified a characteristic weather pattern associated with these regional dust storms that involved an intense surface low pressure system moving quickly across southern Canada coupled with a high pressure system centered over Nevada. In all these events, as the synoptic system weakened, declining wind speeds resulted in cessation of blowing dust in the region. Locations with available average 24-hour PM_{10} concentrations for each event are summarized in Table 3. For the 1993 and 1999 events, hourly averaged PM_{10} concentrations from monitors are presented.

3.3 RESULTS AND DISCUSSION

Predicted PM_{10} concentrations and comparison with measurements for each event are presented in this section. Ideally, predictions should be evaluated with continuous measurements from a dense network of sampling stations to fully resolve spatial heterogeneities and temporal patterns of the dust plume. However, PM_{10} measurements are relatively scarce for this region and only a limited number of measurements was available during each event in this study, hence sub grid spatial and temporal heterogeneities not simulated by the model may contribute to uncertainties in comparing model results to just a few observation points.

Emission fluxes and PM_{10} mass concentrations are discussed in units of kg km^{-2} hr^{-1} and mg m^{-3}, respectively. Units of g km^{-2} hr^{-1} and μg m^{-3} are utilized for low emission

fluxes and PM_{10} concentrations. Unless explicitly stated, discussions are in Pacific Standard Time (PST).

3.3.1. November 23, 1990 and October 21, 1991

On November 23, 1990, the prevailing winds were southwesterly and in Kennewick (KW), wind speeds exceeded 9.0 m s^{-1} throughout the morning. In Yakima County, predicted maximum average 24-hour PM_{10} concentration was 6.7 mg m^{-3} (Figure 3). In KW and Rockwood (RW), observed average 24-hour PM_{10} concentrations were 251 and 126 µg m^{-3}, respectively and while these concentrations were overpredicted with observed to predicted concentrations ratios of 0.53 in KW and 0.76 in RW (Table 4), the overall magnitude of the event was reasonably well predicted.

For the October 21, 1991event, maximum wind speeds in Spokane were 19.5 m s^{-1} in southerly to southwesterly flow. Figure 4 presents the predicted average 24-hout PM_{10} concentrations with a maximum concentration of 0.6 mg m^{-3} in Lincoln County. This event was underpredicted at Crown Zellerbach (CZ), Millwood (MW), RW and KW with observed to predicted concentrations ratios ranging from 6 to 12 (Table 4). In general, this underestimation could be due to errors associated with predicting the meteorology and emissions in the source regions.

3.3.2. September 11 and November 3, 1993

On September 11, a low-pressure system was centered over Canada resulting in strong southwesterly surface winds in the Pacific Northwest with concentrations exceeding 2000 µg m^{-3} in Spokane [*Claiborn et al.,* 1998]. Maximum PM_{10} emissions were 5 kg km^{-2} s^{-1},

predicted to occur in Grant and Douglas Counties and this resulted in a maximum average 24-hour PM_{10} concentration of 6.9 mg m^{-3} in Douglas County (Figure 5). This result differs from *Claiborn et al*. [1998], who identified KW and the surrounding areas as the dust source for this event. It is expected that the results in the current study would be more accurate due to the improvements by *Chandler et al.* [2002] to D in EMIT-PM. In general however, PM_{10} concentrations were underpredicted at all the sampling locations (Table 4).

Predicted hourly concentrations were evaluated against hourly averaged PM_{10} concentrations measured with a Tapered Element Oscillating Microbalance (TEOM). The error bars on Figure 6 reflect the standard deviation obtained from averaging the concentrations in nine 4 km by 4 km grid cells surrounding the location of the sampling station. Elevated PM_{10} concentrations in Figure 6 were observed from 0500 and the peak at 1600 coincided with maximum wind speeds of 12 m s^{-1}. The maximum PM_{10} concentration of 0.5 mg m^{-3} was under predicted and displaced temporally but the relative magnitudes of the maximum and minimum concentrations were well simulated.

In the November 3, 1999 event, PM_{10} emissions were predicted to exceed 2000 kg km^{-2} s^{-1} in Klickitat County and advection from the source region resulted in maximum PM_{10} concentrations of 8.5 mg m^{-3} in Umatilla County (Oregon) (Figure 7). Observed to predicted average 24-hour PM_{10} concentration ratios at the sampling stations indicate excellent agreement (1.0 to 2.5; Table 4). Figure 8 shows a comparison of the hourly averaged observed and predicted concentrations at RW. Wind speeds at RW remained elevated above 8.0 m s^{-1} until 1300, which matches the patterns in the observed PM_{10} concentration peaks. Even though the maximum PM_{10} concentration appears to be displaced temporally by

approximately 6 hours, as with the September 11, 1993 event, the relative magnitudes of maximum and minimum PM_{10} concentrations are well represented.

3.3.3. August 30, 1996

This event was unique as it occurred in the summer season. The source region was identified in Douglas County, with maximum PM_{10} emissions of 7.4 mg m^{-3}. Predicted average 24-hour PM_{10} concentrations at RW and CZ were 1.2 and 0.95 μg m^{-3}, vastly underpredicted from the observed concentrations of 212 and 128 μg m^{-3} at RW and CZ, respectively (Table 4). This was the smallest event simulated in terms of strength of wind and duration of the storm. Further analysis of the simulation problems with this event is discussed in Section 4.

3.3.4. September 23 - 25, 1999

The large dust storm events of September 1999 occurred over a three-day period with PM_{10} concentrations near source regions in Umatilla County predicted to be 6.3 mg m^{-3} on September 23 and 0.5 mg m^{-3} on September 25. Predicted and observed hourly concentrations at KW and CZ are presented in Figures 10 and 11, respectively. In general, simulations captured the onset of the dust event in Kennewick (Figure 10), which occurred on September 25 but failed to predict the observed peak concentrations of 1.7 mg m^{-3} at 1200 on September 23. The maximum predicted concentration for this 3-day event was 3.0 mg m^{-3} on September 24 at 2300, predicted to occur 2 hours ahead of the observed maximum for that period, which was 1.7 mg m^{-3} at 0100, September 25. Comparisons made

against observations during periods when observed concentrations exceeded 80 μg m^{-3} (Table 4) resulted in a reasonable observed to predicted ratio of 0.78.

In Spokane (Figure 11), the model predicted the onset of elevated PM_{10} concentrations on September 23, even though the predicted maximum concentration of 0.1 mg m^{-3} at 1900 is an underestimation of the observed maximum concentration of 0.4 mg m^{-3}, which occurred three hours later at 2200. On September 25, observed maximum PM_{10} concentration of 1.5 mg m^{-3} occurred at 1000 corresponding to maximum wind speeds of 15.4 m s^{-1}, whereas the predicted maximum was 0.7 mg m^{-3} at 0500. The statistical comparison of model predictions to observed concentrations for Spokane are presented in Table 4. For Spokane, the model underestimated PM_{10} concentrations by a factor of almost 2.6, even though the overall distribution trend was fairly well represented. The model also failed to predict the magnitude of the maximum observed concentration and the timing of its occurrence. However, it is encouraging to note that the observed to predicted PM_{10} concentration ratios for both KW and Spokane are well within the overall range of values obtained for the previous events, with the exception of the August 30, 1996 event.

3.4 SUMMARY OF MODEL PERFORMANCE

Table 5 is a summary of the statistics detailing the performance of the modeling system against observed meteorological observations for each event. To compute the statistics, 20 surface stations, representing urban and rural areas, were chosen for each event, except for the September 1999 event, for which only 9 surface stations were available. These measurements are hourly averages from a network of meteorological stations and were incorporated into CALMET to improve model predictions and therefore, these tests are not

independent verifications of the model performance. However, they are valuable tools to utilize as an overall representation and analyses of the wind speeds and wind directions.

The statistical tests applied are index of agreement (D), mean error (ME) and mean absolute error (MAE). D and MAE are measures of the correlation of the predicted and measured time series and ME is a measure of the mean bias in the predictions. Ideally, D should be 1 and MAE should be the smallest value possible to reflect excellent agreement between the observed and predicted values. A positive value for ME reflects an overprediction whereas a negative value implies that the data has been underpredicted.

The best overall model performance in terms of meteorological predictions was the September 23 to 25, 1999 event. D for both wind speeds and wind directions were > 0.95 MAE for wind directions was < 7 º. For all the other events, D for wind speeds ranged from 0.60 to 0.80 and for wind directions, ranged from 0.30 to 0.70. The overall deviation of the predicted from observed wind speeds ranged from 0.1 to 2.0 m s^{-1}. Wind directions for the August 30, 1996 event were poorly predicted, as reflected in the large MAE value (70 º). The wind speeds for this event were also the most underpredicted (ME = -0.3 m s^{-1}), even though the agreement between the predicted and observed wind speeds and directions were higher compared to most of the other events.

Table 6 is an overall summary of the six modeled events in this study, tabulated against several factors, including the predicted average 24 hour wind speeds, percentage of cell-hours when wind speeds exceeded the pre-determined threshold wind speed of 5.5 m s^{-1}, maximum observed PM_{10} concentrations and the ratio of observed to predicted PM_{10} concentrations. The maximum observed PM_{10} concentration highlights the maximum concentration recorded by a sampling station during each dust storm event over the course of

24 or 72 hours. The values in the last column of Table 6 show the average observed to predicted PM_{10} concentration ratios (for all stations) for each event.

The first four events in Table 6 were strong dust storm events with average wind speeds ranging from 6.1 to 7.8 m s^{-1}, corresponding to a significant amount of the cells within the erodible region predicted to have winds sustained above 5.5 m s^{-1} for the 24 hour duration. These strong events were also characterized by high concentrations of PM_{10} observed at the sampling stations. For three of the events presented in Table 6, the ratios of observed to predicted concentrations are less than 2 which is quite good in comparison to the amount of calibration required in previous simulations with this system [*Claiborn et al.*, 1998, *Lee* 1998]. In the remaining events, the ratios are 3.7, 6.5 and 155, which indicates significant underestimation of the observed PM_{10} levels. Given the fact that the observed and predicted wind speeds are in good agreement, the results for the events suggest either errors in predicting the occurrence of emission, i.e. too high threshold velocity or error in the plume transport direction, i.e. the plume misses the receptors.

These potential sources of errors were analyzed in the context of the August 30, 1996 event. From the statistical analyses, wind directions for this event were the most inaccurately represented (MAE = 6.6 º) and while correlation between measured and predicted wind directions (D) was not the lowest, it could certainly have compounded the effect of maintaining a non-varying U_{te} at 5.5 m s^{-1}. *Xuan and Sokolik* [2002] successfully utilized a constant threshold wind speed to identify dust sources in Northern China but studies [*Draxler et al.*, 2001] have shown that parameterizing this variable to roughness parameters to different soil classes would be more representative and future improvements to EMIT-PM should consider this aspect.

In EMIT-PM, U_{te} was determined through visual observations to range from 4.4 to 6.6 m s $^{-1}$ and is linearly parameterized to PM_{10} flux in the emissions algorithm. Decreasing U_{te} to 4.4 m s $^{-1}$ increased PM_{10} concentrations for the August 30, 1996 event by 30 to 50 %. Another important emission variable is WC and increasing soil dryness (WC values approaching 1 in several land use categories) and hence, soil erosivity, resulted in a 20 to 40 % increase in PM_{10} emissions, mainly from dry fallow lands. However, even though the overall intensity of the event increased with decreasing U_{te} and increasing WC, the receptors in the August 30, 1996 event were still not significantly impacted by the dust plume due to the predicted wind directions which were consistently towards the southeast in the modeling domain (Figure 9). The overall results suggest the model performed better at predicting PM_{10} concentrations of large events characterized by average wind speeds exceeding 5.5 m s $^{-1}$ and PM_{10} concentrations exceeding 300 μg m $^{-3}$. *Draxler et al.* [2001] also observed this trend in their model, which successfully predicted large-scale events (> 1000 μg m $^{-3}$) while overpredicting small-scale events (100 to 200 μg m $^{-3}$).

Table 7 presents the amount of PM_{10} emitted in the modeling domain as a function of the different land use categories for each event. The September 23 to 25, 1999 event resulted in the largest PM_{10} emissions (74 Gg), with approximately 95 % from DF lands. Among the dust storms that lasted 24 hours whereas, the November 23, 1990 event resulted in the largest PM_{10} emission at 30 Gg, with approximately 61 % from DF lands and 37 % from IRR lands. These emissions represent a significant loss of fine particles and nutrient content from the agricultural regions in eastern Washington. The August 30, 1996 event had the lowest PM_{10} emission at 2.3 Gg. In general however, the average loss of PM_{10} soil for a 24-hour dust storm event in eastern Washington (excluding the August 30, 1996 event) was 22 Gg. In

terms of contribution towards the global dust loading, an average regional dust storm from eastern Washington represents about 0.5 to 1 % of the global daily average dust flux (based an estimated 1604 Tg yr^{-1} for 0.1 – 6 μm radius particles, from *Ginoux et al.* [2001]).

Besides improving meteorological predictions and PM_{10} emission parameterizations, it is also important to express soil emissions algorithm in terms of key variables most likely to change as agricultural practices evolve under the stress of adapting to new economic trends and technologies. In eastern Washington, since DF lands are the largest contributors among all the landuse categories to dust emissions and conversion to DC or CRP should reduce the erosivity of the soil, especially during occasions of high wind speeds. However, increasing the surface cover and/or wetness on DF lands may also reduce erosivity potentials by a comparable magnitude. In the Southern High Plains of the US, which is a source of dust during periods of high wind events, *Stout and Lee* [2003] documented a decline of 18 % in the fraction of potentially erodible cropland between 1982 and 1987. They attributed this decline to the introduction of CRP in 1986, which may have led to a reduction in reported hours of blowing dust from 1985 to 1987. The capability to predict the effects of evolving agricultural practices on dust emission is certainly vital to avoid adverse impacts on regional air quality.

3.5 CONCLUSIONS

The CP^3 windblown dust modeling system with the incorporation of MM5 and MCIP2 was applied to simulate six major dust storm events to predict dust source locations in eastern Washington, quantify PM_{10} emissions during a dust storm event and PM_{10} concentrations in downwind urban areas. PM_{10} emissions were estimated based on soil type and land use data

common to regions practicing dry land agriculture, with incorporation of other aspects including soil moisture, roughness length and threshold wind velocities. This study employed a more consistent approach to modeling meteorology, which is the main driver to windblown dust events and the subsequent transport and dispersion of the emitted PM_{10}, than our previous modeling studies.

Parameterization of various soil characteristics in the emission model was generally accurate and is reflected in the excellent agreements between predicted and modeled PM_{10} concentrations (less than 2) for three of the dust storm events; November 23, 1990, November 3, 1993 and September 23 to 25, 1999. The October 21, 1991 and September 11, 1993 events were underpredicted with corresponding observed to predicted PM_{10} concentration ratios of 6.5 and 3.7, respectively. The August 30, 1996 event was poorly represented with a corresponding observed to predicted PM_{10} concentration ratio of 155. Even though these ratios are based on observations from a limited number of sampling stations in Benton and Spokane counties, this range of ratios reflects the inherent complications associated with accurate predictions of plume width and directions, which are correlated to the size of a dust storm event. In terms of fine particle emissions, PM_{10} emissions ranged from an average of 21 Gg for a 24-hour dust storm event to 74 Gg for a 72-hour dust storm event.

The ability to simulate individual dust episodes and identify potential dust regions is an important aspect of regional models. In terms of global dust loading, windblown dust from agricultural regions are potentially important contributions, and results from high-resolution models could be used to complement global scale models, which generally have horizontal resolutions in the range of 4 to 5 ° and thus, are unable to replicate daily and seasonal

evolution of dust emissions, transport, deposition and turbidity near dusty regions [*Tegen* 2003]. Employing even higher horizontal resolutions (e.g. 1 km) may improve sub grid heterogeneities due to wind field variabilites but will require much improved parameterizations of emission factors such as threshold wind speeds, soil surface cover, roughness elements and soil water content. However, higher resolution models would also aid in improving identification of dust sources and quantifications of fine particles emissions. These aspects should be considered in future studies.

ACKNOWLEDGEMENTS

This work has been supported by the USDA ARS Columbia Plateau (CP^3) PM_{10} project. We would like to thank Dr. Joseph Vaughan at WSU and Dr. Susan O'Neill, U. S. Forest Service, Seattle, WA for their invaluable assistance with this work. We would also like to thank all the members of the CP^3 project for their cooperation.

(Tables and Figures follow references)

REFERENCES

Alfaro, S. C., and L. Gomes, Modelling mineral aerosol production by wind erosion: Emission intensities and aerosol distributions in source areas, *J. Geophys. Res.*, *106*, 18075 – 18084, 2001

Chandler, D. G., K. E. Saxton, J. Kjelgaard, and A. J. Busacca, A technique to measure fine-dust emission potentials during wind erosion, *J. Soil Sci. Soc. Am.*, *66*, 1127 – 1133, 2002.

Claiborn, C., B. Lamb, A. Miller, J. Beseda, B. Clode, J. Vaughan, L. Kang, and C. Newvine, Regional measurements and modeling of windblown agricultural dust: The Columbia Plateau PM_{10} program, *J. Geophys. Res.*, *103*, 19753 – 19767, 1998.

Draxler, R. R., D. A. Gillette, J. S. Kirkpatrick, and J. Heller, Estimating PM_{10} air concentrations from dust storms in Iraq, Kuwait and Saudi Arabia, *Atmos. Environ.*, *35*, 4315 – 4330, 2001.

Dudhia, J., D. Gill, Y.-R. Guo, K. Manning, J. Michalakes, A. Bourgeois, W. Wang, and J. Wilson, PSU/NCAR mesoscale modeling system tutorial class notes and user's guide, *MM5 Modeling System Version 3*, 281 pp., Mesoscale and Microscale Meteorology Division, National Center for Atmospheric Research, Co., 2001.

Elbir, T., Comparison of model predictions with the data of an urban air quality monitoring network in Izmir, Turkey, *Atmos. Environ.*, *37,* 2149 – 2157, 2003.

Fryrear, D. W., J. E. Stout, L. J. Hagen, and E. D. Vories, Wind erosion: Field measurement and analysis, *Transac. of the ASAE*, *34*, 155 – 160, 1991.

Ginoux, P., M. Chin, I. Tegen, J. M. Prospero, B. Holben, O. Dubovik, and S.-J. Lin, Sources and distributions of dust aerosols simulated with the GOCART model, *J. Geophys. Res.*, *106*, 20255 – 20273, 2001.

Gomes, L., J. L. Rajot, S. C. Alfaro, and A. Gaudichet, Validation of a dust production model from measurements performed in semi-arid agricultural areas of Spain and Niger, *Catena*, 52, 257 – 271, 2003.

Horning. L. B., L. D. Stetler, K. E. Saxton, Surface residue and soil roughness for wind erosion protection, *Transac. of the ASAE*, *41*, 1061 – 1065, 1998.

Houser, C. A., and W. G. Nickling, The emission and vertical flux of particulate matter <10 μm from a disturbed clay-crusted surface, *Sedimentology*, *48*, 255 – 267, 2001.

Kim, K. W., Y. J. Kim, and S. J. Oh, Visibility impairment during Yellow Sand periods in the urban atmosphere of Kwangju, Korea, *Atmos. Environ.*, *35,* 5157 - 5167, 2001.

Larney, F. H., M. S. Bullock, S. M. McGinn, and D. W. Fryrear, Quantifying wind erosion on summer fallow in southern Alberta, *J. Soil and Water Cons.*, *50*, 91 – 95, 1995.

Lee, B.-H., Regional air quality modeling of PM_{10} due to windblown dust on the Columbia Plateau, M.S. thesis, Washington State University, Pullman, 1998.

Saxton, K. E., Wind erosion and its impact on off-site air quality in the Columbia Plateau – An integrated research plan, *Transac. of the ASAE*, *38*, 1031 – 1038, 1995.

Saxton, K. E., D. Chandler, L. Stetler, B. Lamb, C. Claiborn, and B.-H. Lee, Wind erosion and fugitive dust fluxes on agricultural lands in the Pacific Northwest, *Transac. of the ASAE*, *43*, 623 - 630, 2000.

Scire, J. S., F. R. Robe, M. E. Fernau, and R. J. Yamartino, *A user's guide for the CALMET meteorological mode (Version 5.0)*, 214 pp., Earth Tech, Inc, 1999.

Scire, J. S., R. J. Yamartino, G. R. Carmichel, and Y. S. Chang, *CALGRID: A Mesoscale photochemical grid model, Vol 11: User's guide*, 178 pp., Prepared for State of California Resources Board, Sacramento, California, 1989.

Stout, J. E., Dust and environment in the Southern High Plains of North America, *J. Arid Env.*, *47*, 425 – 441, 2001.

Stout, J. E. and J. A. Lee, Indirect evidence of wind erosion trends on the Southern High Plains of North America, *J. Arid Env.*, *55*, 43 – 61, 2003.

Tegen, I., Modeling mineral dust aerosol cycle in the climate system, *Quaternary Science Review*, 22, 1821 – 1834, 2003.

Tegen, I., and I. Fung, Contribution to the atmospheric mineral aerosol load from land surface modification, *J. Geophys. Res.*, *100*, 18707 – 18726, 1995.

Tegen, I., and I. Fung, Modeling of mineral dust in the atmosphere: Sources, transport, and optical thickness, *J. Geophys. Res.*, *99*, 22897 – 22914, 1994.

Xuan, J., and I. N. Sokolik, Characterizations of sources and emission rates of mineral dust in Northern China, *Atmos. Environ.*, *36,* 4863 – 4876, 2002.

Yamartino, R. J., J. S. Scire, G. R. Carmichael, and Y. S. Chang, The CALGRID Mesoscale photochemical grid model – I. Model formulation, *Atmos. Environ., 26A*, 1493 – 1512, 1992.

Yu, S., C. S. Zender, and V. K. Saxena, Direct radiative forcing and atmospheric absorption by boundary layer aerosol in southwestern US: Model estimates on the basis of new observations, *Atmos. Environ.*, *35,* 3967 – 3977, 2001.

Table 1. Estimated values for surface cover (SC, %), surface roughness (K, cm), water content (WC, non-dimensionless) and aerodynamic roughness (z_o, cm) in the EMIT-PM model for major land use categories and events. Land use categories are rangeland (RL), irrigated (IRR), dry crop (DC), dry fallow (DF), and conservation resource program (CRP).

Event	Parameters	Landuse categories				
		RL	IRR	DC	DF	CRP
November 23, 1990	SC	70	10	90	15	70
	K	1.8	1.3	1.8	1.3	1.8
	WC	0.1	0.8	0.1	0.5	0.1
	Zo	4	1	5	0.6	4
October 21, 1991	SC	70	25	90	10	70
	K	1.8	1.3	1.8	1.8	1.8
	WC	0.1	0.9	0.3	0.9	0.1
	Zo	4	1	5	0.6	4
September 11, 1993	SC	70	50	90	5	70
	K	1.8	1.3	1.8	2	1.8
	WC	0.1	0.8	0.1	1	0.1
	Zo	4	1	1	0.6	4
November 3, 1993	SC	70	20	90	10	70
	K	1.8	1.3	1.8	1.8	1.8
	WC	0.1	0.9	0.2	0.8	0.1
	Zo	4	1	5	0.6	4
August 30, 1996	SC	70	20	90	5	70
	K	1.8	1.3	1.8	1.3	1.8
	WC	0.1	1	0.1	1	0.1
	Zo	4	1	5	0.3	4
September 23 to 25, 1999	SC	70	50	90	5	70
	K	1.8	1.3	1.8	2	1.8
	WC	0.1	0.8	0.1	1	0.1
	Zo	4	1	1	0.6	4

Table 2. Average soil dustiness (D, dimensionless) and relative erodibility ratio (ER, dimensionless) for the major soil classes on the Columbia Plateau region

Soil classes	D	ER
	Average	Average
DQ	0.50	6.660
DE	0.15	0.250
DS	2.66	0.239
L1A	1.98	1.000
L2A	2.94	0.550
L1B	3.39	0.480
L2B	3.05	0.320
L3	3.39	0.360
L4	4.38	0.420
L5	5.47	0.140

Table 3. Location of surface stations and summary of available PM_{10} measurements for each event

Stations	Location and description			Dust storm events
	Latitude (N)	Longitude (W)	Description	
Crown Zellerbach (CZ)	47.66	117.36	Industrial, Spokane	October 21, 1991; September 11, 1993; November 3, 1993; August 30, 1996; September 23-25, 1999
Rockwood (RW)	47.75	117.41	Residential, Spokane	November 23, 1990, October 21, 1991; September 11, 1993; November 3, 1993; August 30, 1996
Millwood (MW)	47.69	117.28	Light commercial, Spokane	October 21, 1991; November 3, 1993
Spokane Auto Glass (SAG)	47.63	117.53	Urban, Spokane	September 11, 1993; November 3, 1993
Turnbull (TB)	47.36	117.61	Wildlife refuge, SW of Spokane	September 11, 1993
Kennewick (KW)	46.21	119.14	Urban, Kennewick	November 23, 1990; October 21, 1991; September 11, 1993; November 3, 1993; September 23-25, 1999

Table 4. Summary of observed and predicted 24-hour PM_{10} average concentrations

Locations	Observed PM_{10} ($\mu g\ m^{-3}$)	Predicted PM_{10} ($\mu g\ m^{-3}$)	Observed / Predicted
November 23, 1990			
RW	251	332	0.76
KW	126	237	0.53
October 21, 1991			
CZ	361	62	5.8
MW	305	59	5.2
RW	267	90	3.0
KW	1035	89	11.6
September 11, 1993			
CZ	300	73.0	4.1
SAG	297	74.5	4.0
RW	255	54.0	4.6
TB	490	106.0	4.6
KW	118	103.0	1.1
November 3, 1993			
CZ	207	82	2.5
SAG	156	95	1.6
MW	176	59	3.0
RW	100	96	1.0
August 30, 1996			
RW	212	1.2	175
CZ	128	0.95	135
September 23 to 25, 1999			
CZ	400	155	2.58
KW	630	808	0.78

Table 5. Summary of meteorological (wind speed, WS (m s^{-1}) and wind direction, WD (°)) performance statistics (index of agreement, D, mean error, ME and mean absolute error, MAE) computed for 20 meteorological stations for the 1990 to 1996 events and 9 meteorological stations for the September 23 to 25, 1999 event.

Event	D		ME		MAE	
	WS	WD	WS	WD	WS	WD
Nov. 23, 1990	0.65	0.70	0.1	11	2.1	19
Oct. 21, 1991	0.79	0.40	0.2	24	1.9	48
Sept. 11, 1993	0.81	0.29	0.3	23	1.7	43
Nov. 3, 1993	0.83	0.27	0.8	-4.3	1.5	32
Aug. 30, 1996	0.80	0.60	-0.3	36	1.6	70
Sept. 23 –25, 1999	0.99	0.95	-0.1	1.0	0.1	6.6

Table 6. Summary of modeled events

Event	24 hour average wind speeds ($m\ s^{-1}$)	% cell-hours (wind speeds > 5.5 $m\ s^{-1}$)	Maximum observed PM_{10} ($\mu g\ m^{-3}$)	Observed / Predicted PM_{10} concentrations
Nov. 23, 1990	7.8	86	332	0.7
Oct. 21, 1991	6.3	17	1035	6.5
Sept. 11, 1993	6.1	46	490	3.7
Nov. 3, 1993	7.3	29	1166	1.9
Aug. 30, 1996	4.1	14	212	155
Sept. 23 to 25, 1999	5.6	34	1731	1.7

Table 7. Predicted PM_{10} emissions (Mg) from land use categories; rangeland (RL), irrigated (IRR), dry crop (DC), dry fallow (DF), and conservation resource program (CRP).

Event	RL	IRR	DC	DF	CRP
Nov. 23, 1990	431	11202	60	18739	38
Oct. 21, 1991	89	1805	37	7247	10
Sept. 11, 1993	140	483	28	13313	22
Nov. 3, 1993	298	7515	99	24031	46
Aug. 30, 1996	12	256	2	2080	2
Sept. 23 to 25, 1999	480	2801	173	70427	61

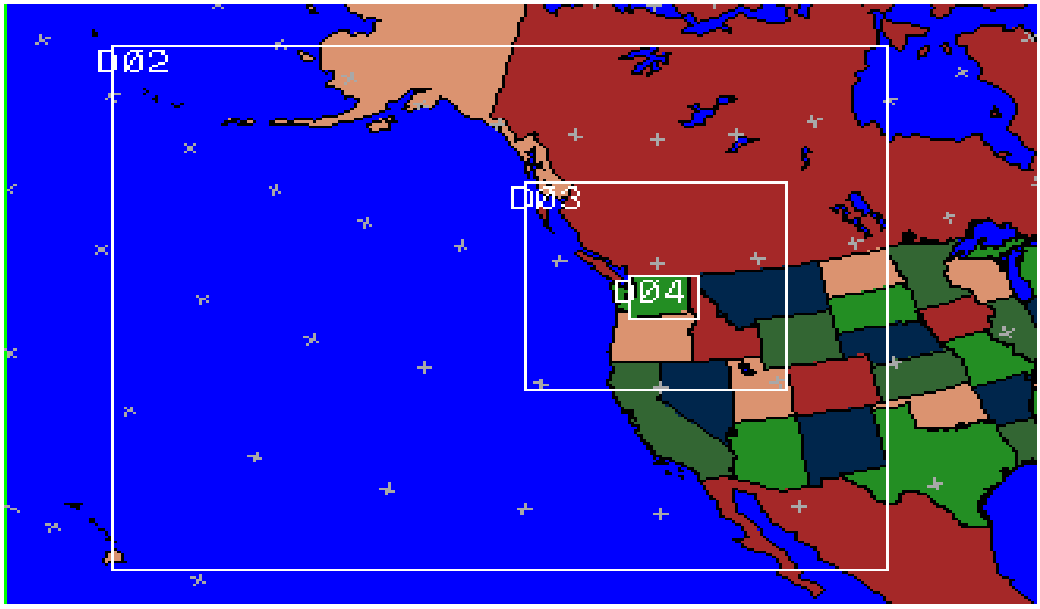

Figure 1. MM5 modeling domain, with nested grids of 36 km, 12 km and 4 km

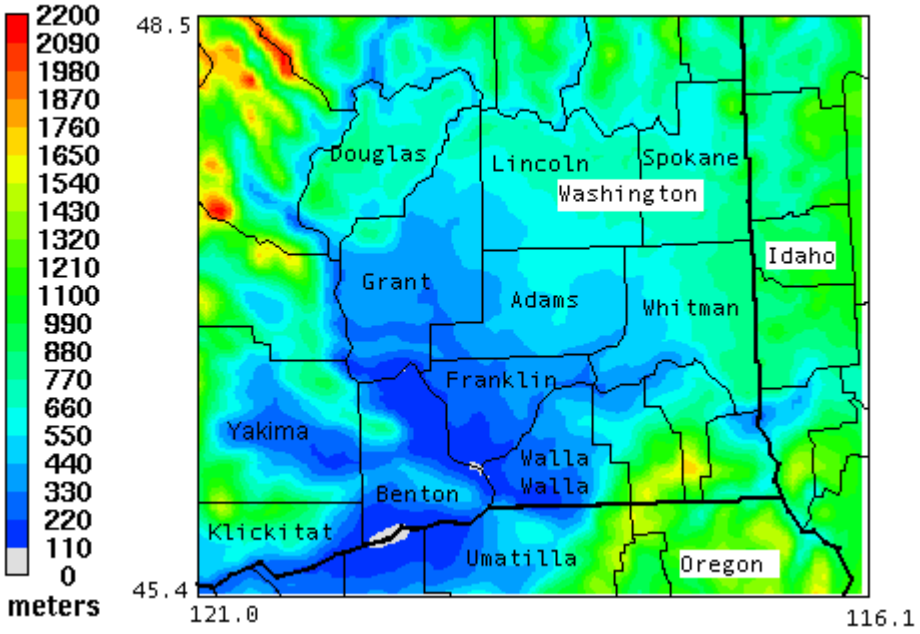

Figure 2. The CALMET model domain and terrain elevation

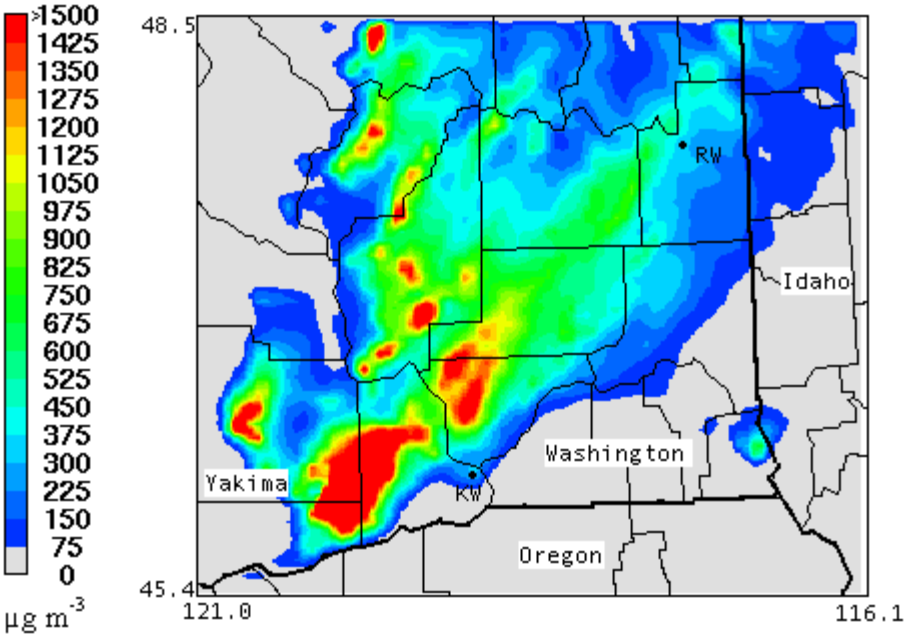

Figure 3. Predicted average 24-hour PM_{10} concentrations, November 23, 1990

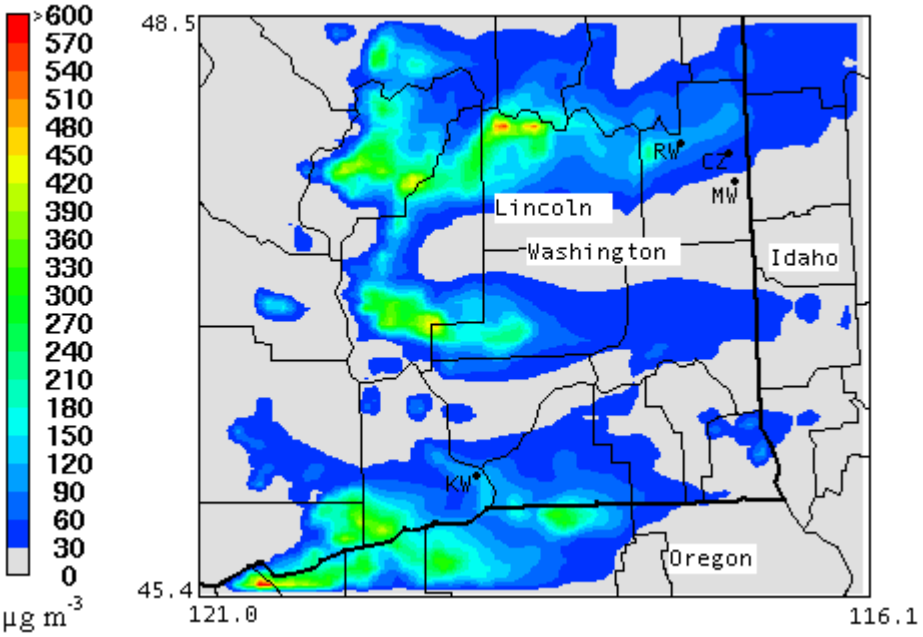

Figure 4. Predicted average 24-hour PM_{10} concentrations, October 21, 1991

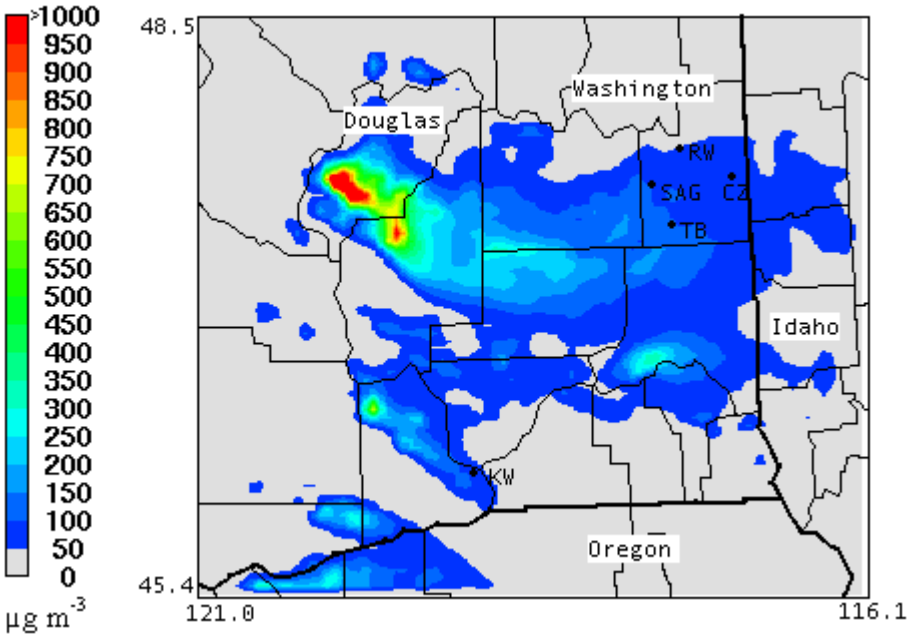

Figure 5. Predicted average 24-hour PM_{10} concentrations, September 11, 1993

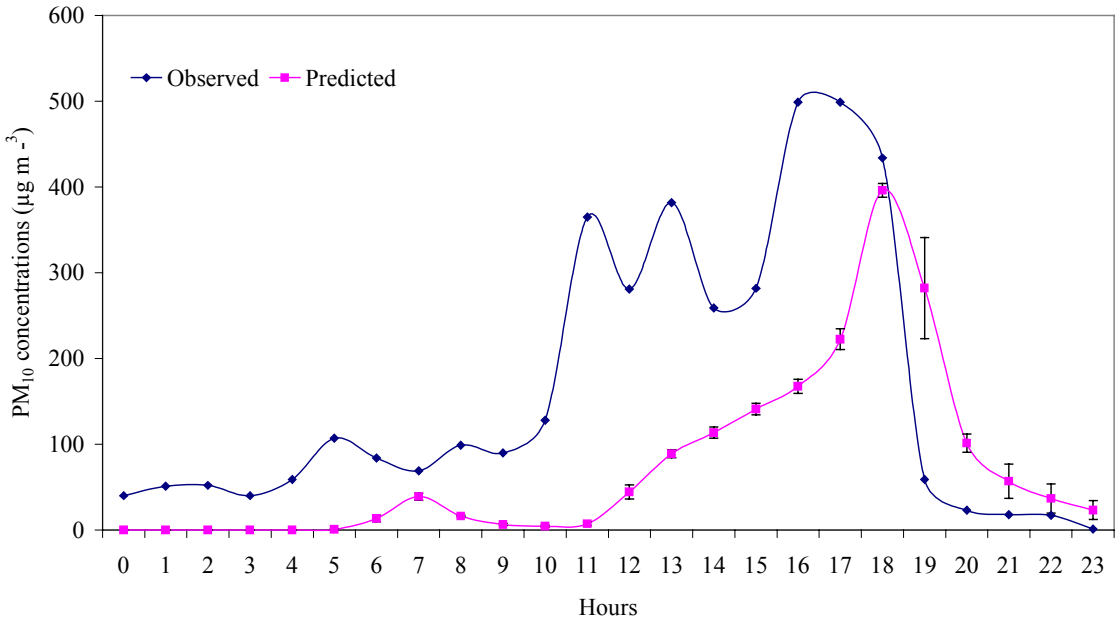

Figure 6. Predicted and measured PM_{10} concentrations at CZ, September 11, 1993

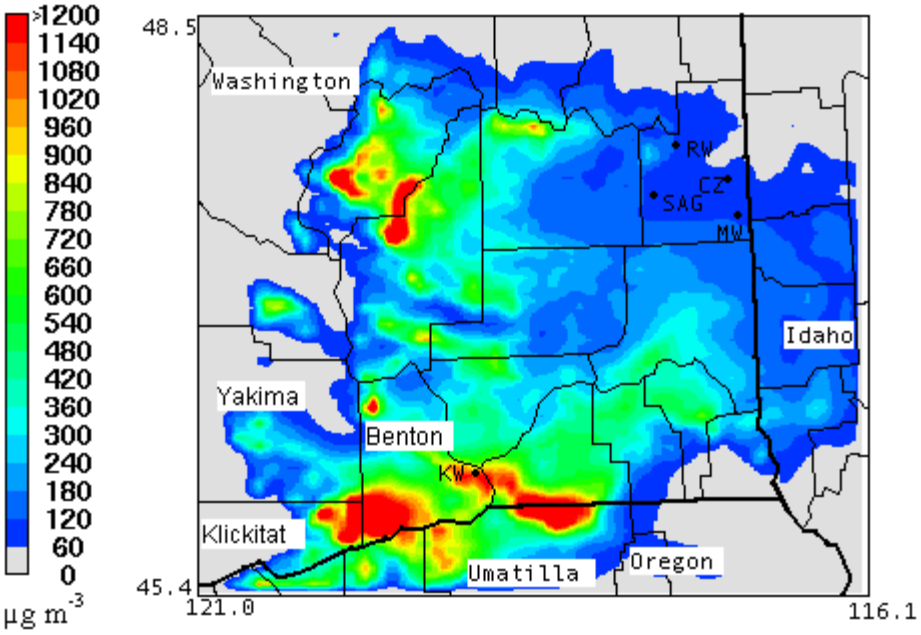

Figure 7. Predicted average 24-hour PM_{10} concentrations, November 3, 1993

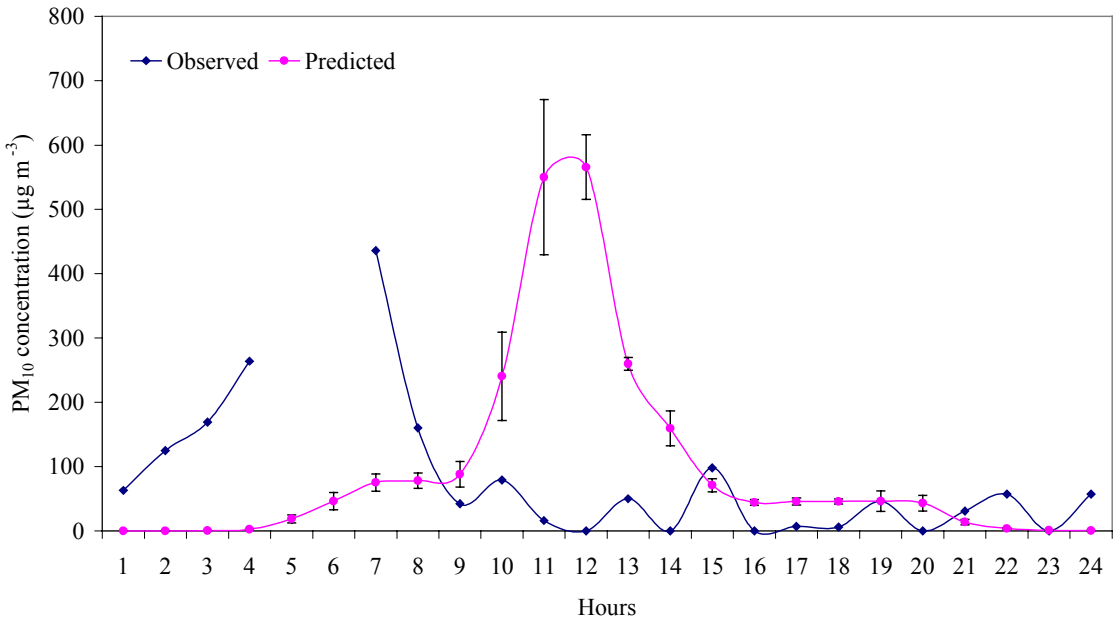

Figure 8. Predicted and measured PM_{10} concentrations at RW, November 3, 1993

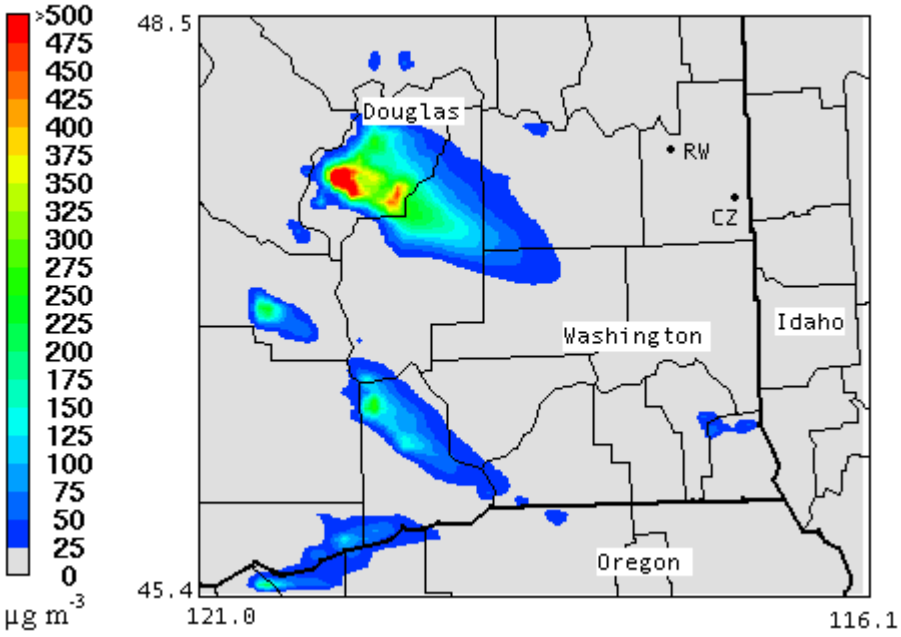

Figure 9. Predicted average 24-hour PM_{10} concentrations, August 30, 1996

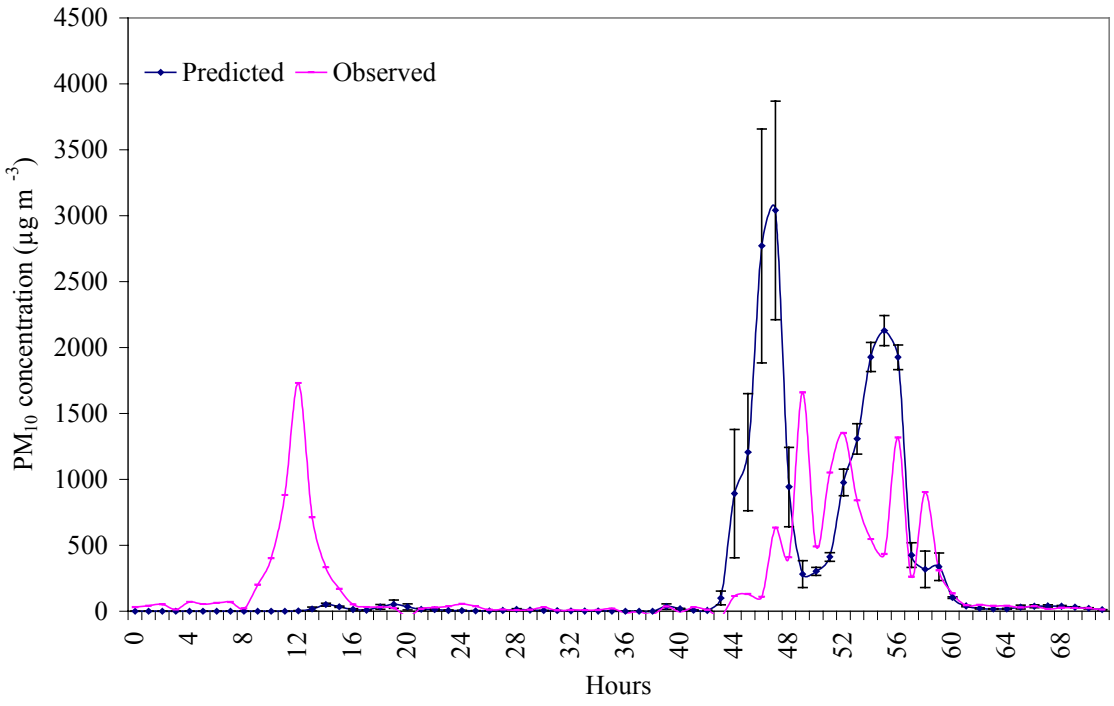

Figure 10. Predicted and measured PM_{10} concentrations at KW, September 23 to 25, 1999

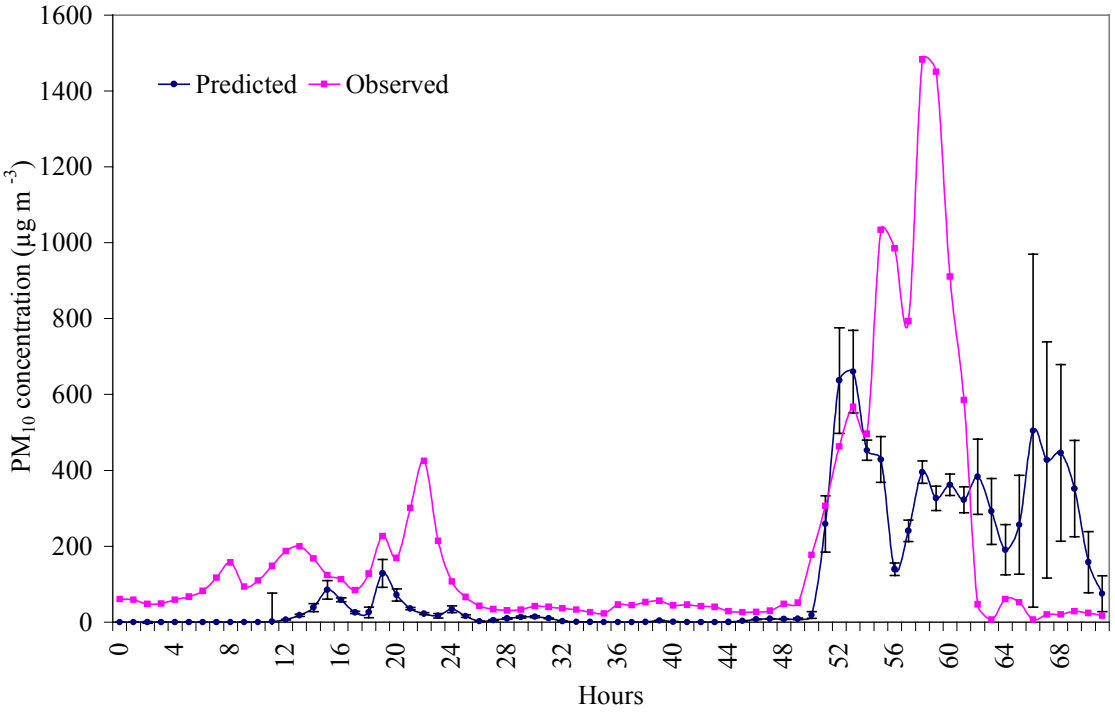

Figure 11. Predicted and measured PM_{10} concentrations at CZ, September 23 to 25, 1999

Chapter 4

Sensitivity of a regional windblown dust model to uncertainties in PM_{10} emission parameters

Sensitivity of a regional windblown dust model to uncertainties in PM_{10} emission parameters

Irra Sundram*, Brian Lamb, and Candis Claiborn

Laboratory for Atmospheric Research

Department of Civil & Environmental Engineering

Washington State University

Pullman 99164, Washington

USA

*** Corresponding author.**

E-mail address: irra_t-mohanasu@wsu.edu

Tel.: + 1-509-335-6248

Fax.: + 1-509-335-7632

ABSTRACT

Variables influencing the emission of fine dust from semi-arid agricultural regions in eastern Washington have been explicitly parameterized in an emissions model, EMIT-PM. This model has been incorporated with Eulerian meteorological and dispersion models to predict PM_{10} concentrations due to windblown dust in the region (Sundram et al., 2004). In the current study, EMIT-PM was numerically evaluated to test the sensitivity of predicted PM_{10} emissions and concentrations due to uncertainties in the emission input parameters from different land use categories and soil classes in eastern Washington. Simulations were executed for a dust storm event which occurred from September 23 to 25, 1999. PM_{10} emissions varied by a factor of 2 for the modeling domain of 107008 km^2 due to uncertainties in threshold wind speeds and by 67 % due to uncertainties in the surface roughness of dry fallow lands, which represent highly erodible surfaces. Predicted emissions were not very sensitive to the aerodynamic roughness length. Wind erosion control strategies based on modifications to farming practices were also identified and evaluated in terms of predicted PM_{10} concentrations in down wind populated areas. The fractional amount of vegetative surface cover and the area coverage of dry fallow land with respect to dry crop land were varied as potential control strategies. Reducing the area coverage of dry fallow lands by 40 % resulted in PM_{10} concentrations decreasing by a factor of 2 to 3 in down wind locations and hence, this strategy appeared to provide significant improvements even with respect to the large variations in emissions due to uncertainties in the characterization of threshold wind speeds.

Keywords: Wind erosion, dust, vertical flux, sensitivity, Washington

4.1 INTRODUCTION

In semi-arid agricultural regions, wind erosion is a serious problem that leads to loss of fertile soil and degradation of air quality due to blowing dust. The magnitude of wind erosion is influenced by many factors such as topography, elevation, vegetative cover, soil type, soil surface texture and microclimate (Weinan et al, 1996; Horning et al., 1998; Houser and Nickling, 2001). Agricultural practices can have a significant effect on the potential for wind erosion within a region. Identifying agricultural methods that minimize the down wind impact of agricultural wind erosion while maintaining or improving economic efficiency is a major focus of the Columbia Plateau PM_{10} program in the Pacific Northwest (Saxton, 1995).

Most wind erosion research has utilized portable wind tunnels on agricultural lands either individually or in combination with field dust samplers to quantify the influences of surface wetness, aerodynamic and random roughness lengths and vegetative surface cover on soil fluxes (Weinan et al., 1996; Horning et al., 1998; Saxton et al., 2000; Rajot et al., 2003; Gomes et al., 2003a; Zhang et al., 2004). However, explicit parameterization of these complex interactions in dust production models is inherently complicated since emissions are sensitive to combinations of various parameters. For example, in sandy agricultural soil, Rajot et al. (2003) found that roughness heights were more effective for erosion control compared to surface crusting. In silty soils, Zhang et al. (2004) suggested that aerodynamic roughness height was an important aspect of erosion control. In semiarid regions, Li et al. (2001) found that pebble mulch could reduce wind erosion by 84 to 96 %. Lopez (1998) indicated that temporal changes of various characteristics, especially threshold friction velocities, influenced vertical dust fluxes and should be accounted for in dust emission models.

Dust emission models have been developed for numerical evaluation of vertical dust fluxes on regional scales. Gomes et al. (2003b) tested the ability of their empirically developed dust production model (DPM) to predict PM_{20} emissions from two field locations in Spain and Niger and found reasonable agreement with measurements. Draxler et al. (2001) constructed an emissions model for predicting PM_{10} emissions in southwestern Asia. The windblown dust emissions were incorporated into a Lagrangian transport and dispersion model, which produced accurate prediction of major dust storm events, although PM_{10} concentrations were over-predicted at low concentrations.

In the Pacific Northwest, we have developed a semi-empirical PM_{10} emissions model (EMIT-PM) as part of a regional air quality modeling system developed through the Columbia Plateau PM_{10} project (Saxton, 1995; Claiborn et al., 1998; Saxton et al., 2000; Chandler et al., 2002). Claiborn et al. (1998) described the initial development of this windblown dust modeling system, which consists of EMIT-PM, the MM5 and CALMET meteorological models and a Eulerian grid model, CALGIRD; Lee (1998) reported initial results using the EMIT-PM dust emission scheme for five historical dust events. Modifications to EMIT-PM by Saxton et al. (2000) and Chandler et al. (2002) resulted in more accurate parameterizations of the various soil properties embedded in the horizontal and vertical dust flux algorithms, and these improvements were evaluated for six dust storms by Sundram et al. (2004) who found that the revised modeling system matched observed PM_{10} concentrations to a much better degree, especially for larger dust storms, than in the Lee (1998) study. For three large events, the observed to predicted PM_{10} concentration ratios at most sampling locations in eastern Washington were less than 2 (Sundram et al., 2004).

The underlying motivation of this study is to ascertain the sensitivity of the modeling system to uncertainties associated with the emission parameters embedded in EMIT-PM. These analyses are essential for evaluations of the overall robustness of the emissions model and potential wind erosion control strategies that could be implemented by the agricultural community. In the first phase, empirically determined values for soil surface crusting and wetness (WC), soil surface roughness (K), aerodynamic roughness heights (zo), vegetative surface cover (SC), erodibility index (EI) and the threshold wind velocity (U_t) were varied systematically to test the resultant sensitivity of PM_{10} emissions. In the second phase, the potential effects of changes in farming practices on dust emissions and resulting changes in PM_{10} concentrations were evaluated. The dust control strategies involved varying the amount of vegetative surface cover (SC) on each land use type and increasing the area coverage of dry crop land with respect to dry fallow land. A detailed description of EMIT-PM, derivations of the final algorithm utilized for PM_{10} emissions computations and the methodology employed for the sensitivity analyses are presented in Section 4.2. Section 4.3 presents results from both parts of the sensitivity analyses and Section 4.4 concludes this paper with summary and conclusions.

4.2 PM_{10} EMISSIONS MODEL

4.2.1 EMIT-PM algorithms

There are two main algorithms in EMIT-PM: the horizontal and vertical fluxes of soil (Saxton et al., 2000). The horizontal dust movement, Q_T (kg m^{-1}) is parameterized as a function of the wind energy (W_T, g s^{-2}) and surface properties:

$$Q_T = W_T * EI * (e^{-0.05 * SC}) * (e^{-0.52 * K}) * WC \quad (1)$$

where W_T and EI are expressed as,

$$W_T = \rho * \Sigma U^2 (3m) * (U (3m) - U_t) \Delta t \quad (2)$$

$$EI = 0.06 * (ER^{0.6}) \quad (3)$$

In the term W_T, ρ is the air density (1.2×10^{-3} g m $^{-3}$), U (3m) represents the wind speed (m s $^{-1}$) at 3 m and U_t is the threshold wind velocity (m s $^{-1}$) for soil mobilization (defined as 5.5 m s $^{-1}$ by Saxton et al., 2000). W_T is summed over the number of measurement intervals (Δt, s) for which U (3m) > U_t (Saxton et al., 2000). EI, the erodibility index ((kg m $^{-1}$)(g s $^{-2}$) $^{-1}$), represents the intrinsic susceptibility of tilled soil to erosion when wind erosion protection measures are not implemented. EI is computed from the relative erodibility ratio, ER (dimensionless), which defines the erosivity potential obtained through wind tunnel trials performed for each soil class. The surface roughness, K (cm) is defined through visual observations in test plots; SC, the surface cover is defined as the percentage of flat residue; WC is a non-dimensional index from 0 – 1 describing the degree of wetness and crusting of the soil.

The vertical dust flux, F_D (g m $^{-2}$ s $^{-1}$) is expressed as a function of the horizontal dust flux, soil dustiness coefficient (D, dimensionless) and aerodynamic roughness, zo (cm).

$$F_D = K_f * U_* * Q_T * D (\Delta t)^{-1} \quad (4)$$

where

$$K_f = \text{compilation of empirical constants, (g s)(kg m}^2)^{-1} \quad (5)$$

$$U_* = \frac{U(3m) * 0.4}{\log(\frac{300}{zo})} \quad (6)$$

SC, WC, K, and zo were characterized from wind tunnel and field measurements for five land use categories: rangeland (RL), irrigated land (IRR), dry crop (DC), dry fallow (DF) and

conservation resource program (CRP) lands (Saxton, 1995; Saxton et al., 2000). Mean values for D and ER were determined through wind tunnel and laboratory experiments for 10 soil classes of varying degrees of erosivity, common to the Washington, Idaho and Oregon regions (Saxton et al., 2000). The parameterized values for SC, K, WC, zo, D and ER are presented in Sundram et al. (2004).

By substituting the relevant terms into equation (4), F_D is expressed as:

$$F_D = \frac{Cv * (U^4(3m) - U^3(3m) * U_t) * (ER^{0.6}) * \exp(-0.05 * SC) * \exp(-0.52 * K) * D * WC}{\log(\frac{300}{zo})} \quad (7)$$

Cv encompasses the all the constants from Eqs. (2) to (6) (kg s^3 m^{-6}). The parameterizations in Eq. (7) allow for preliminary analytical evaluations of the relationships between F_D and the emission parameters. With the exception of WC, the dependence of FD on Ut, ER, SC, K and zo is non-linear in nature, suggesting that the sensitivity of PM_{10} emissions to these parameters over spatially inhomogeneous terrains can only be adequately characterized through numerical methods. The linear relationship between F_D and WC imply a constant rate of change in PM_{10} emissions with change in WC. In general, PM_{10} emissions are positively correlated to increases in WC and ER, which represent increasingly erodible conditions but are negatively correlated to increases in the parameters SC, K and zo, which represent greater erosion protection for the soil.

4.2.2 Approaches to sensitivity analyses

The test case utilized in this study was a large dust storm that occurred on September 23 to 25, 1999. The meteorology for the 72-hour simulation period was simulated through MM5 and CALMET for a domain ranging from 45.425 N to 48.479 N and 121.000 E to

116.105 E and the details are presented in Sundram et al. (2004). These models have horizontal resolutions of 4 km x 4 km for a total of 88 x 76 grids (longitude x latitude). EMIT-PM was employed to simulate the mass of PM_{10} emitted as functions of perturbations applied individually and simultaneously to the various PM_{10} emission parameters. The ranges of values over which these parameters are valid were obtained through field and wind tunnel measurements by Saxton et al. (2000). To investigate the effectiveness of dust control strategies stemming from modifications to farming practices, CALGRID was employed to simulate the transport and dispersion of PM_{10} from agricultural source regions and PM_{10} concentrations at two down wind populated communities, Crown Zellerbach in Spokane (CZ, 47.65 N, 117.32 E) and Kennewick (KW, 46.21 N, 119.36 E).

4.3 RESULTS

4.3.1. Sensitivity of PM_{10} emissions to key parameters

PM_{10} emissions were predicted for U_t values ranging from 4.4 to 6.6 m s^{-1}, where lower velocities represent soil with lower binding energies. The maximum PM_{10} emission for the domain was 100 Gg when U_t was 4.4 m s^{-1}, and a minimum of 51 Gg was predicted at 6.6 m s^{-1} (Table 1). For each incremental increase (1 m s^{-1}) in U_t, PM_{10} emissions decreased at an average rate of 22.2 ± 6.3 Mg / (m s^{-1}), and was well represented by a linear relationship (R^2 = 99 %). Most of the PM_{10} emitted (~ 95 % of total emissions) was from the highly erodible dry fallow lands. Perturbations to ER were implemented over a range of values defined by the ratio of the sensitivity case to the base case $R_{ER} = ER_s / ER_b$: 0.2, 0.5, 1.0, 1.5, and 1.8, where 1.0 represents the base case value for ER. The maximum PM_{10} emission was 84 Gg at R_{ER} = 1.8 and the minimum emission was 63 Gg at R_{ER} = 0.1 (Table

1). The average rate of change in PM_{10} emissions as R_{ER} varied from 0.2 to 1.8 was 0.258 ± 0.028 Mg / (% change in ER) and was well represented by a positively correlated linear relationship (R^2 = 99 %).

The effects on PM_{10} emissions from individual perturbations in SC, K, WZ and zo are also summarized in Table 1. SC, K and zo are parameterized to be inversely correlated with total dust production whereas an increase in WC indicates increasing susceptibility to wind erosion (Horning et al., 1998; Saxton et al., 2000). Dry fallow lands were the largest dust emitters (≥ 90 %) and the overall maximum PM_{10} emission of 97 Gg was predicted at K = 1.5 cm (Table 1) and minimum PM_{10} emissions were 58 Gg, at K = 2.5 cm which implies that K has a more significant effect on the degree of wind erosion compared to the other parameters. This result is corroborated by Horning et al. (1998) who established the importance of K and SC in reducing wind erosion) through their field study with portable wind tunnels. CRP lands were the least sensitive to these parameters, where the mean difference between maximum and minimum PM_{10} emissions was 65 Mg. In terms of the regression equations, the most prominent feature was the strong correlation (R^2 > 95 %) obtained in all categories. These numerical simulations appear to indicate that on a regional scale, PM_{10} emissions were linearly dependent on K and WC whereas in some land use categories, SC and zo were better represented by exponential trends.

The sensitivity of PM_{10} emissions to perturbations applied simultaneously to each emission parameter over the entire modeling domain was also investigated. The values in Figure 1 represent the emitted PM_{10} mass, summed over all land use categories, as a function of the different degrees of perturbations applied to the emission parameter. At R_{ER} = 1.0, PM_{10} emissions for the modeling domain were fairly consistent across all emission

parameters, with a mean emission of 74.2 ± 0.4 Gg (Figure 1). Perturbations to WC from R_{ER} of 0.2 to 1.8 resulted in the largest variation in total PM_{10} emissions of ~55 Gg. There was a large spike in emissions when WC values were increased from 1.5 to 1.8 and this was due to an approximately 31 % increase in emissions from DF lands. This spike could be due to the existence of a threshold soil wetness level associated with the crusting effect for DF lands. Incremental increases in SC and K resulted in PM_{10} emissions decreasing at a fairly constant rate of 0.11 ± 0.015 Mg / (% change in SC) and 0.38 ± 0.081 Mg / (% change in K), respectively.

Perturbations to zo did not appear to have a significant effect on PM_{10} emissions and the mean value across the entire range (0.2 to 1.8) was 74 Gg ± 2.2 Gg. This is in contrast to sensitivity tests by Alfaro et al. (2003) who found that PM_{20} emissions from the DPM model were greatly influenced by zo. However, the effect of crusting which may be more significant in fine textured soil, common to the eastern Washington region, was not factored in the DPM. The relationship between zo and total dust production was linear for the range of values in this study (zo minimum = 0.3 cm) and this trend was partly supported by wind tunnel trials conducted by Zhang et al. (2004) who found that a non-linear relationship was apparent only at values smaller than 0.1 cm.

In summary, the sensitivity range associated with predicted PM_{10} emissions for the 72-hour dust storm was relatively large from 62 to 117 Gg for an area of 107008 km^2. Uncertainties in the parameterization of U_t resulted in a factor of 2 variations in PM_{10} emissions for the modeling domain whereas uncertainties in the values of SC, WC and K resulted in PM_{10} emissions from dry fallow lands varying by 7 Gg, 28 Gg and 39 Gg respectively. These results can be applied to considerations of wind erosion control

strategies. While the degree of crusting, parameterized in WC, is a dominant influence on erosion processes in semi-arid regions, it does not translate to an economically feasible erosion control strategy. However, increasing SC and / or K, especially on DF lands, through vegetative windbreaks, standing residues and conservation crop rotations, are certainly compatible with current farming methods (Nordstrom and Hotta, 2004).

4.3.2. Sensitivity of PM_{10} emissions to farming practices

Perturbations to SC were simulated in EMIT-PM and CALGRID at R_{ER} = 0.2, 0.5, 1.0, 1.5, 1.8, and 2.0, where 1.0 represents the base case value for SC in each land use category. In terms of PM_{10} emissions, maximum emissions were predicted at SC = 0.2 (~78.8 Gg) and minimum emissions at SC = 2.0 (~69 Gg). A similar trend was observed for PM_{10} concentrations in KW and CZ (Figure 2) where the largest decrease in PM_{10} concentrations, represented by the maximum difference in concentrations defined between R_{ER} = 0.2 and 2.0 (Δ PM_{10} maximum), was 100 μg m^{-3} predicted at hour 52 in CZ and 380 μg m^{-3} at hour 47 in KW. These results suggest average decreases in PM_{10} concentrations (evaluated between R_{ER} = 1.0 and 2.0) of 7.5 % in CZ and 8.5 % in KW, which are barely discernible improvements with respect to the sensitivity of PM_{10} emissions to variations in SC (~10 - 11 %). However, increasing both surface cover and roughness on dry fallow lands could result in more significant erosion protection.

To evaluate the effect of converting dry fallow lands into cropped lands, perturbations were applied to the percentage of DF land coverage with respect to DC land, which was 50 %:50 % for the base case. PM_{10} emissions were evaluated for DF: DC ratios of 40 %:60 %, 30 %:70 %, 20 %:80 % and 10 %:90 % (Figure 3). PM_{10} emissions had a non-linear rate of

decrease as DF lands were converted to DC lands and the maximum reduction in emissions (from DF: DC of 50%: 50% to 10%: 90%) was 49 Gg (Figure 3). Figure 4 presents the concentration difference between 50 %:50 % and 10 %:90 % and Δ PM_{10} maximum in CZ was 282 μg m^{-3} (hour 67) and 2320 μg m^{-3} (hour 47) in KW. Through this erosion control strategy of converting DF lands to DC lands, PM_{10} concentrations at CZ and KW were reduced by a factor of > 2 and > 3, respectively. These are significant improvements even with current uncertainties in the parameterizations of U_t resulting in large variations of PM_{10} emissions (e.g. factor of 2).

In summary, both these approaches, increasing SC or converting DF to DC lands, were predicted to be effective in reducing PM_{10} concentrations at both urban locations. However, these analyses suggest that PM_{10} concentrations downwind to emissions are more sensitive to the second management strategy, which involves converting DF lands to DC systems. The larger Δ PM_{10} maximum with this approach could be attributed to the fact that fallow lands often define dust source regions and implementing cropping systems on these lands will significantly reduce its erosivity.

4.4 CONCLUSIONS

A semi-empirical dust production model designed to evaluate PM_{10} emissions from agricultural fields in eastern Washington was developed as part of the Columbia Plateau PM_{10} project. Evaluations were carried out to test the sensitivity of the various PM_{10} emission parameters. The largest variations in PM_{10} emissions were predicted to occur from uncertainties in the parameterization of U_t (± 1 m s^{-1}) and from dry fallow lands due to K (± 0.5 cm), which suggest the need for more controlled and detailed field experiments to obtain

representative values for these parameters. PM_{10} emissions were least sensitive to variations in zo, which may be attributed to the properties of the fine textured soils in this region and CRP lands were fairly insensitive to perturbations applied to any of the emission parameters.

The air quality impacts of two feasible wind erosion control strategies were investigated and evaluated at two down wind populated locations. The first strategy involved increasing SC for all land use categories from 10 % to 100 % over the empirically determined range and this resulted in a maximum PM_{10} decrease of 380 μg m^{-3} which was barely significant with respect to the sensitivity of the model to uncertainties in the parameterization of SC. However, the second strategy which involved converting dry fallow lands into crop (DC lands) resulted in predicted PM_{10} reductions of 2320 μg m^{-3} when the area coverage of DF lands was decreased from 50 to 10 %. These improvements in PM_{10} concentrations were significantly higher that the magnitude of uncertainties associated with the parameterizations of U_t.

These results show that even though EMIT-PM was parameterized through linear multipliers of various empirically determined emission parameters (Eq. 7), the overall sensitivity of PM_{10} emissions in a domain from perturbations to these parameters necessitate considerations of the intricate relationships between different land use and soil types. Wind erosion control practices should emphasis site-specific strategies that target land use types already susceptible to erosion, which could include increasing the amount of vegetative soil cover left on fallow lands, roughness conditions and the amount of irrigation implemented in a cropping cycle. This study also gives an indication of the sensitivity of EMIT-PM to variations in threshold wind speeds, surface cover and surface wetness and crusting, when numerically integrated over a large heterogeneous area. Even though values for the

emissions parameters utilized in this study were empirically determined in representative field conditions, PM_{10} emissions were predicted to vary by as much as 200 % due to uncertainties in the values of some emission parameters, illustrating the need for careful evaluations of the input data prior to utilization in regional scale numerical models.

ACKNOWLEDGEMENTS

This work has been supported by the USDA ARS Columbia Plateau (CP^3) PM_{10} project. We would like to thank all the other members of the CP^3 project for their invaluable contributions.

(Tables and Figures follow references)

REFERENCES

Alfaro, C.A., Rajot, J.L., Nickling, W., 2003. Estimation of PM20 emissions from wind erosion: Main sources of uncertainties. Geomorphology, 59, 63 - 74.

Chandler, D.G., Saxton, K.E., Kjelgaard, J., Busacca, A.J., 2002. A technique to measure fine-dust emission potentials during wind erosion. Journal of Soil Science Society America 66, 1127–1133.

Claiborn, C., Lamb, B., Miller, A., Beseda, J., Clode, B., Vaughan, J., Kang, l., Newvine, C., 1998. Regional measurements of modeling of windblown agricultural dust: The Columbia Plateau PM_{10} Program. Journal of Geophysical Research 103, 19753–19767.

Draxler, R.R., Gillette, D.A., Kirkpatrick, J.S., Heller, J., 2001. Estimating PM_{10} air concentrations from dust storms in Iraq, Kuwait and Saudi Arabia. Atmospheric Environment 35, 4315–4330.

Gomes, L., Arrúe, J.L., López, M.V., Sterk, G., Richard, D., Gracia, R., Sabre, M., Gaudichet, A., Frangi, J.P., 2003a. Wind erosion in a semiarid agricultural area of Spain: The WELSONS project. Catena 52, 235–256.

Gomes, L., Rajot, J.L., Alfaro, S.C., Gaudichet, A., 2003b. Validation of a dust production model from measurements performed in semi-arid agricultural areas of Spain and Niger. Catena 52, 257–271.

Horning, L.B., Stetler, L.D., Saxton, K.E., 1998. Surface residue and soil roughness for wind erosion protection. Transactions of the ASAE 41, 1061–1065.

Houser, C.A., and Nicking, W.G., 2001. The emission and vertical flux of particulate matter <10 μm from a disturbed clay-crusted surface. Sedimentology 48, 255–267.

Lee, B.-H., 1998. Regional air quality modeling of PM_{10} due to windblown dust on the Columbia Plateau. Masters thesis, Washington State University, Pullman, WA.

Li, X.–Y., Liu, l.-Y., Gong, J.-D., 2001. Influence of pebble mulch on soil erosion by wind and trapping capacity for windblown sediment. Soil & Tillage Research 59, 137–142.

López, M.V., Sabre, M., Gracia, R., Arrúe, J.L., Gomes, L., 1998. Tillage effects on soil surface conditions and dust emission by wind erosion in semiarid Aragón (NE Spain). Soil & Tillage Research 45, 91–105.

Nordstrom, K.F., and Hotta, S., 2004. Wind erosion from cropland in the USA: a review of problems, solutions and prospects. Geoderma, 121, 157 – 167.

Rajot, J.L., Alfaro, S.C., Gomes, L., Gaudichet, A., 2003. Soil crusting on sandy soils and its influence on wind erosion. Catena 53, 1–16.

Saxton, K., Chandler, D., Stetler, L., Lamb, B., Claiborn, C., Lee, B.-H., 2000. Wind erosion and fugitive dust fluxes on agricultural lands in the Pacific Northwest. Transactions of the ASAE 43, 623–630.

Saxton, K.E., 1995. Wind erosion and its impact on off-site air quality in the Columbia Plateau – An integrated research plan. Transactions of the ASAE 38, 1031–1038.

Sundram, I., Claiborn, C., Strand, T., Lamb, B., Chandler, D., Saxton, K., 2004. Numerical modeling of windblown dust in the Pacific Northwest with improved meteorology and dust emission models. Accepted for publication in Journal of Geophysical Research, copyright 2004 American Geophysical Union.

Weinan, C., Zhibao, D., Zhenshan, L., Zuotao, Y., 1996. Wind tunnel test of the influence of moisture on the erodibility of loessial sandy loam soils by wind. Journal of Arid Environment 34, 391–402.

Zhang, C.-L., Zou, X.-Y., Gong, J.-R., Liu, L.-Y., Liu, Y.-Z., 2004. Aerodynamic roughness of cultivated soil and its influences on soil erosion by wind in a wind tunnel. Soil & Tillage Research 75, 53–59.

Table 1

Total PM_{10} emissions in the modeling domain from perturbations to surface cover (SC, %), random roughness (K, cm), surface wetness and crusting (WC, dimensionless) and aerodynamic roughness (zo, cm)

Categories	Range	Maximum total production (Gg)	Minimum total production (Gg)	Regression curve	R^2 (%)
U_t	4.4 – 6.6 [a]	100	51	Mass = -22.907*U_t + 196.10	99
ER	0.2 – 1.8 [b]	84	63	Mass = 11.623*ER + 61.670	99
SC					
Rangeland	56-84	74	74	Mass = 74.361exp (-0.0003*SC)	97
Irrigated	40-60	76	73	Mass = 75.655exp (-0.0019*SC)	98
Drycrop	72-108	74	74	Mass = 74.144exp (-0.0001*SC)	95
Dryfallow	4-6	78	71	Mass = -0.3510*SC + 77.834	99
CRP	56-84	74	74	Mass = -0.0032*SC + 73.995	97
K					
Rangeland	1.3-2.3	74	74	Mass = -0.0252*K + 74.093	99
Irrigated	0.8-1.8	75	73	Mass = -0.1470*K + 74.829	99
Drycrop	1.3-2.3	74	74	Mass = -0.0090*K + 73.996	99
Dryfallow	1.5-2.5	97	58	Mass = -3.8050*K + 98.807	99
CRP	1.3-2.3	74	74	Mass = -0.0032*K + 73.960	99
WC					
Rangeland	0.01-0.2	74	74	Mass = 0.0480*WC + 73.461	100
Irrigated	0.7-0.9	74	74	Mass = 0.0350*WC + 73.556	100
Drycrop	0.01-0.2	74	74	Mass = 0.0173*WC + 73.768	100
Dryfallow	0.8-1.0	88	60	Mass = 1.4090*WC + 58.447	100
CRP	0.01-0.2	74	74	Mass = 0.0061*WC + 73.880	100
zo					
Rangeland	1.5-6.5	74	74	Mass = -0.0068*z_o + 74.021	98
Irrigated	0.5-1.5	74	74	Mass = 74.137exp (-0.0002*z_o)	99
Drycrop	0.5-1.5	74	74	Mass = -0.0024*z_o + 73.965	99
Dryfallow	0.3-0.9	77	71	Mass = 77.415exp (-0.004*z_o)	99
CRP	1.5-6.5	74	74	Mass = -0.0009z_o + 73.952	98

[a] In units of m s^{-1}

[b] Ratio = $\frac{\text{ER (sensitivity case)}}{\text{ER (base case)}}$

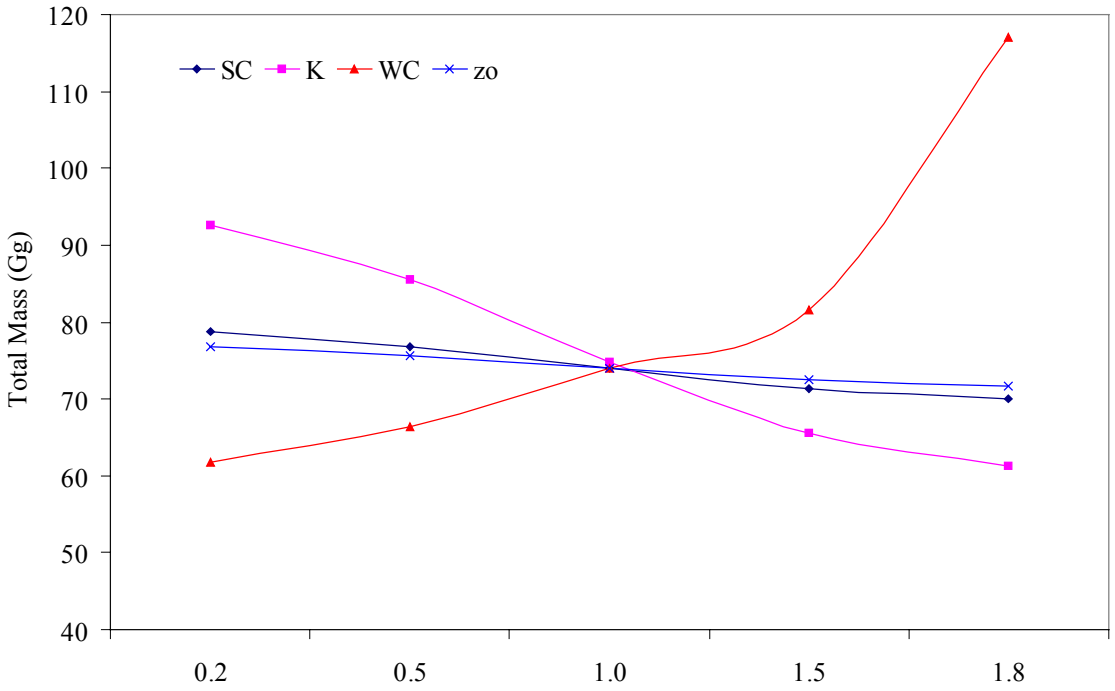

Figure 1. Predicted total PM_{10} emissions in the modeling domain from perturbations (ratio of sensitivity to base case) to surface cover (SC, %), random roughness (K, cm), surface wetness and crusting (WC, dimensionless) and aerodynamic roughness (zo, cm) applied across all land use categories

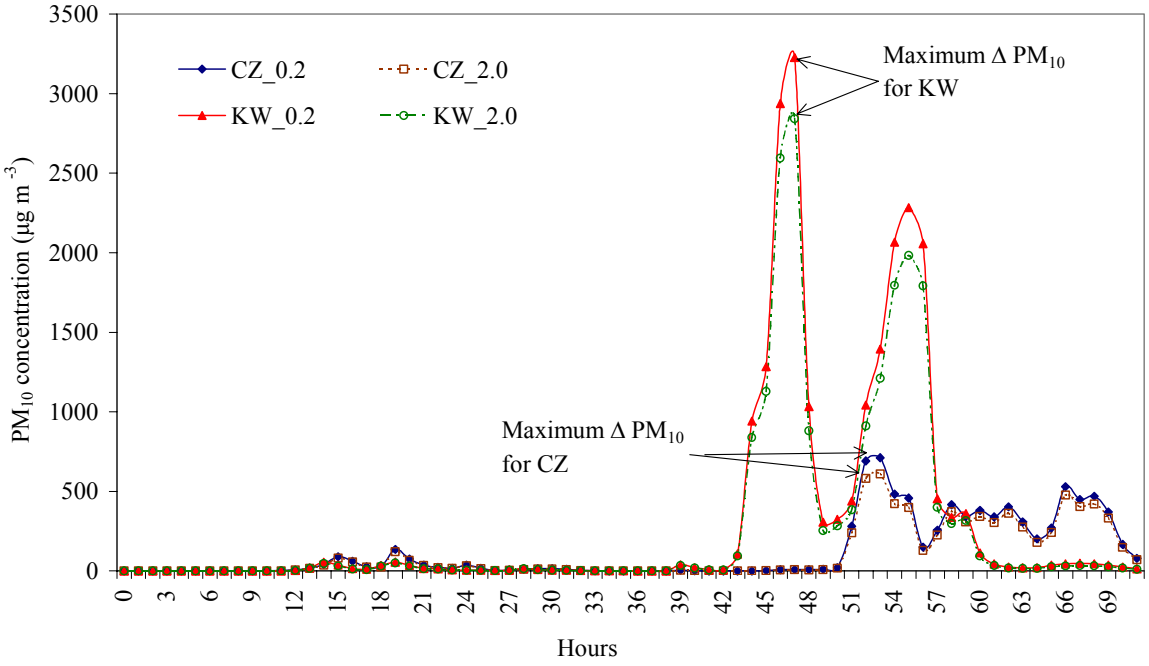

Figure 2. Predicted PM_{10} concentrations in Crown Zellerbach (CZ) and Kennewick (KW) due to perturbations applied to vegetative surface cover (SC)

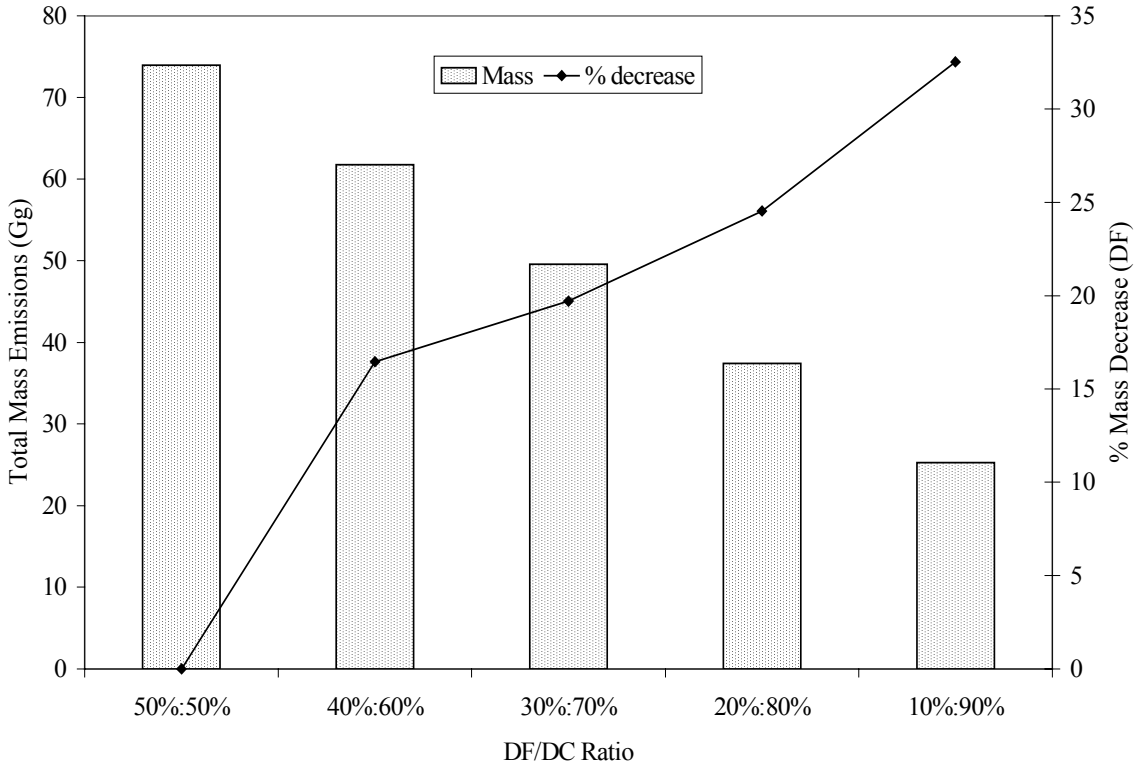

Figure 3. Predicted PM_{10} emissions as a function of perturbations applied to the area coverage of dry fallow (DF) lands with respect to dry crop (DC) lands

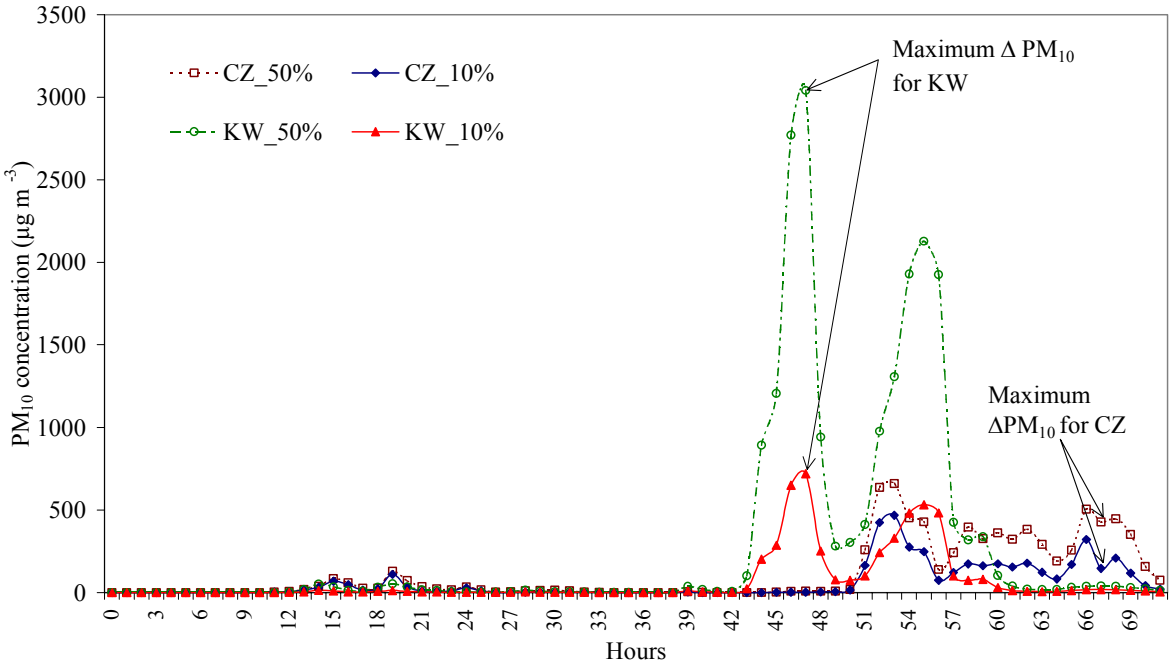

Figure 4. Predicted PM_{10} concentrations in Crown Zellerbach (CZ) and Kennewick (KW) due to perturbations applied to the area coverage of dry fallow (DF) lands with respect to dry crop (DC) lands

Chapter 5

Modeling Aerosol Optical Depths During Episodes of Windblown Dust From Semiarid Agricultural Regions

Modeling Aerosol Optical Depths During Episodes of Windblown Dust From Semiarid Agricultural Regions

Irra Sundram, Candis Claiborn, Brian Lamb

Laboratory for Atmospheric Research,

Department of Civil and Environmental Engineering,

Washington State University,

Pullman, 99164, Washington

Rachel Sampang

2106 Homewood Pl.

Fullertown, CA, 92833 -1202

ABSTRACT

Atmospheric turbidity was modeled for September 11, 1993 and September 23 to 25, 1999 at two urban locations in eastern Washington. During these periods, large regional dust storms, originating from a combination of high wind speeds and erodible agricultural fields, resulted in high PM_{10} concentrations at Spokane and Kennewick in eastern Washington. Aerosol optical depth (AOD) and the Angstroms turbidity parameter, β, were predicted utilizing a numerical modeling system that included the MM5 meteorological model, a PM_{10} windblown dust emission model and the CALGRID regional transport and dispersion model. The optically active size fraction of the suspended dust was assumed to range from 0.1 to 3.0 μm (radius). Lack of ground based radiometric measurements necessitated validation through temporal correlations of the predicted β and observed PM_{10} concentrations time series at downwind populated areas for each event. Correlation coefficients ranged from 0.5 to 0.8. The maximum predicted AOD values ranged from 0.3 to 0.7; these are comparable to values in the published literature. Sensitivity analyses were conducted with respect to size fractionation of fine and coarse particles and extinction coefficients. These analyses indicated that the potential error margin in the modeled AOD values were in the range of ± 10 % to ± 30 %. The model results provide estimates of the magnitude and temporal patterns of AOD during large individual dust storms. This information could be incorporated into general circulation models and used in studies on regional atmospheric circulation effects from dust storms originating from agricultural regions.

5.1 INTRODUCTION

Estimating perturbations to global and regional radiative balances from the interactions of mineral dust in the atmosphere is dependent on accurate quantifications of dust loadings, transport and deposition, microphysical properties such as the size range and optical properties such as the refractive index [*Tegen* 2003]. Due to the temporal and spatial variability of these properties, frequent measurements of dust emissions from source regions, downwind concentrations and turbidity have to be performed to complement predictions from transport and dispersion models in order to constrain radiative forcing predictions.

Turbidity, which is a dimensionless measure of aerosol loading in a vertical column of atmosphere, is characterized by aerosol optical depth (AOD) and the Angstrom turbidity indices (α, β). AOD is an important indicator of the radiative properties of aerosol and is defined as the total normalized column extinction from the direct beam due to absorption and scattering by atmospheric aerosols [*Zakey et al.*, 2004, *Masmoudi et al.*, 2003]. Measured AOD values (500 nm) have exceeded 3.0 in dust plumes originating from the desertified Owens Lake in California [*Niemeyer et al.*, 1999]. In South Korea, radiometric measurements of AOD (500 nm) during the 1999 – 2001 period recorded an increase from a spring background average of 0.45 to greater than 0.70 in dust storm events originating from inland China [*Ogunjobi et al.*, 2004].

The relationship between AOD and wavelength can be used to compute the Angstrom parameters: α is related to aerosol size distribution and approaches very small or even negative values in high wind events dominated by large dust particles, whereas β, which is correlated to the particle concentration in the atmosphere and represents AOD at 1000 nm, typically ranges from 0.0 to 0.5 [*Zakey et al.*, 2004, *Masmoudi et al.*, 2003, *Cachorro et al.*,

2001, *Martinez-Lozano et al.*, 1998]. *Masmoudi et al.* [2003] recorded a minimum α value of – 0.13 corresponding to a maximum β value of 1.52 during the month of June in Tunisia and attributed these results to the influence of dust bearing winds from the Saharan region. *Esposito et al.* [2004] found maximum β values of 0.14 corresponding temporally to the lowest α value of 0.94 during measurements in South Italy.

To assess the impact of turbidity on global radiative budgets, general circulation models have been utilized to simulate global AOD distributions. Using a tracer transport model developed at the NASA Goddard Institute for Space Studies, *Tegen and Fung* [1994] obtained seasonal maximum AOD averages of 0.4 to 0.5, which were underpredicted compared to satellite retrieved AOD values of 0.6 to 1.0 over oceanic regions. *Chin et al.* [2002] and *Ginoux et al.* [2001] compared AOD predictions from the Georgia Institute of Technology-Goddard Global Ozone Chemistry Aerosol Radiation and Transport (GOCART) model with satellite retrieval products and obtained reasonable agreements in high turbidity regions (AOD > 0.2). However, the low spatial resolutions in these models usually prevent successful predictions of individual dust storm events with high turbidities.

The intent of this study was to predict AOD and β for individual dust storm events originating from dryland agricultural practices in eastern Washington by utilizing an integrated numerical modeling system that included meteorological, PM_{10} emission, and transport models. This regional windblown dust modeling system was initially developed to investigate the degradation of air quality due to high PM_{10} associated with regional dust storms [*Sundram et al.*, 2004, *Claiborn et al.*, 1998]. AOD predictions were evaluated qualitatively with other model studies and quantitatively with observed PM_{10} concentrations and sensitivity analyses. The paucity of radiometric measurements, which are ground-based

measurements from sunphotometers or skyradiometers in the modeling domain during these events precluded stringent analytical comparisons. Even so, these predictions provide important estimates of the magnitude and temporal evolution of turbidity parameters in individual, regional scale dust storms originating from dry land agriculture. Detailed temporal variations of AOD with meteorological factors are also discussed in this paper.

5.2 TURBIDITY DATA AND ALGORITHMS

AOD is related to the dust mass loading and extinction parameter by

$$\text{AOD}(\lambda) = \sum_i 0.75 * Q_{ext}(\lambda, r_i) * M_i * f_i * (r_i * \rho_i)^{-1}, \quad (1)$$

where Q_{ext} is a geometry factor dependent on the wavelength λ and effective particle radius, r_i, M_i is the column loading for each particle size class, i, and ρ_i is the mass density for each size class, i [*Chin et al.*, 2002, *Ginoux et al.*, 2001, *Tegen and Lacis*, 1996, *Tegen and Fung*, 1994]. Q_{ext} values were calculated for λ = 400 to 600 nm in 10 nm increments for six size classes using the Mie theory for a complex refractive index (CRI) of 1.53 – 0.0078i, which has been used to represent mineral dust in other studies [*Chin et al*, 2002, *Ginoux et al.*, 2001]. These six size classes (in terms of radii) were 0.1 – 0.18 μm, 0.18 – 0.3 μm, 0.3 – 0.6 μm, 0.6 – 1 μm, 1 – 1.8 μm and 1.8 – 3 μm and r_i in each size class was 0.15 μm, 0.25 μm, 0.4 μm, 0.8 μm, 1.5 μm and 2.5 μm, respectively [*Ginoux et al.*, 2001, *Tegen and Lacis*, 1996]. This conservative approach of considering only particles ≤ 3 μm (radius) as being optically active was employed to avoid poor representation in the Mie scattering range, mainly from increased side scattering [*von Hoyningen-Huene et al.*, 1999]. Classes 1 to 4 were categorized as clay with a mass density of 2.5 g cm $^{-3}$ and classes 5 to 6 were defined as silt with a mass density of 2.65 g cm $^{-3}$ [*Ginoux et al.*, 2001].

M_i was calculated for each size class from PM_{10} concentrations predicted by an empirically based PM_{10} emissions model coupled with meteorological models (MM5 and CALMET) and an Eulerian transport and dispersion model (CALGRID) for 13 vertical layers in the atmosphere (*Sundram et al*., 2004). Due to the lack of more detailed information, the mass fraction in each size class (f_i) was estimated from *Tegen and Lacis* [1996] as 1 %, 4 %, 12 %, 31 %, 32 % and 13 % for size classes 1 to 6, implying approximately 93 % of the PM_{10} is less than 6 μm in diameter and ~ 30 % is less than 2.5 μm in diameter.

The Angstrom parameters are related to the AOD by

$$AOD\ (\lambda) = \beta\ \lambda^{-\alpha} \tag{2}$$

where λ is defined in μm [*Esposito et al.*, 2004, *Masmoudi et al.*, 2003, *Adeyefa and Holmgren*, 1996]. β and α can be obtained by taking the logarithm of equation (2), which results in equation (3)

$$\ln (AOD) = -\ \alpha \ln\ \lambda + \ln \beta \tag{3}$$

The predicted AOD at the corresponding λ were fitted to a straight line to produce a single value of α and β for each hour. The use of β in this context differs from the original definition of β at 1 μm, but is supported by the recommendations of *Martinez-Lozano et al.* [1998] who showed that parameterizing measurements at β = 1 μm to obtain AOD values led to lower correlation coefficients compared to parameterizations within a spectral range of 400 to 670 nm (UV-VIS range).

The two dust storm events modeled in this study occurred on September 11, 1993 and from September 23 to 25, 1999. Both these events were characterized by high wind speeds and resulted in violations of PM_{10} air quality standards (> 150 μg m^{-3}) in several urban areas in eastern Washington, namely in the greater Spokane area and Kennewick [*Sundram et al.*,

2004, *Claiborn et al.*, 1998]. In this study, the temporal patterns of AOD and β are modeled for two locations: Crown Zellerbach (CZ, 47.66 N, 117.36 W), and Kennewick (KW, 46.21 N, 119.41 W) (Figure 1).

5.3 MODEL VALIDATION AND ANALYSES

The temporal patterns of β, calculated from the predicted AOD for a range of λ from 400 to 600 nm using equation (2), were compared with the observed PM_{10} concentrations. Since β is indicative of dust mass loading in a column of atmosphere, hourly distributions during a dust storm event should be at least temporally correlated to hourly averaged observed PM_{10} concentrations from surface stations. A more analytical comparison will not be very realistic since sub-grid heterogeneities would not have been adequately characterized in model predicted PM_{10} concentrations that were used to compute β [*Tegen* 2003]. Since the size distribution of the suspended dust was pre-determined in the context of this study, α was fairly constant between 0.0 to – 0.4.

Figures 2 and 3 present variations of the observed and predicted PM_{10} concentrations and predicted β at CZ and KW, respectively, for the dust storm event of September 23 to 25, 1999. In Figure 2, the predicted maximum β value of 0.89 (hour 63) for CZ is displaced temporally from the observed maximum PM_{10} concentration of 1483 μg m^{-3} (hour 59). Correlation statistics were used to determine the overall relationship and a correlation coefficient (r) of 0.53 indicates a positive trend between observed PM_{10} concentrations and β, which reflects temporal agreement of periods with increased atmospheric dust loading for CZ. This trend is only slightly better for predicted PM_{10} concentrations and β with a correlation coefficient of 0.57. While the maximum β value (0.89) exceeded the 0.0 to 0.5

range usually associated with this turbidity parameter, higher values (> 2) are not unusual and have been recorded in Tunisia during the influx of Saharan dust [*Masmoudi et al.*, 2003].

In KW (Figure 3), there is a stronger positive temporal trend between predicted PM_{10} and β as reflected by a r of 0.9, compared to a r of 0.55 between observed PM_{10} concentration and β. For this location, the maximum PM_{10} concentration of 1731 μg m^{-3} observed at hour 13, whereas a modest β of 0.04 was predicted at hour 15. The maximum β of 0.5 at hour 56 appears to be correlated to the observed PM_{10} concentration of 1658 μg m^{-3} at hour 50. The September 11, 1993 event occurred over a 24-hour period with maximum observed PM_{10} concentrations of 500 μg m^{-3} at hours 17 and 18 (Figure 4). This peak in atmospheric dust loading coincided well with the maximum β of 0.4 at hour 17 and is reflected by a r of 0.79 between observed PM_{10} concentration and predicted β. The correlation between predicted PM_{10} concentrations and β was only slightly lower at 0.78, indicative of good overall temporal agreement.

Figures 5, 6 and 7 present the temporal patterns and magnitudes of predicted AOD (at 500 nm) for CZ (September 23 to 25, 1999), KW (September 23 to 25, 1999) and CZ (September 11 1993), respectively. Figures 5, 6 and 7 also include observed wind directions and hourly averaged wind speeds from local meteorological stations at the monitoring sites and this allows potential dust source regions to be evaluated from the comparisons of these meteorological parameters and predicted AOD trends. From Figures 5 and 6, maximum AOD values were co-incident with southwesterly wind speeds exceeding 12 m s^{-1}, and suggest that the potential source region could be in Umatilla County, Oregon, which lies southwest to KW and CZ (Figure 1). This prediction corroborates the analyses in *Sundram et al.* [2004] concerning potential source regions for this event. For the September 11, 1993

event (Figure 7), maximum AOD values were associated with north to northwesterly winds exceeding 10 m s^{-1}; these winds were associated with a rapidly moving low-pressure system in Canada [*Claiborn et al.*, 1998]. As suggested in *Sundram et al.* [2004], the source regions appear to be Grant and Douglas Counties, which lie northwest of CZ (Figure 1). In general, the positive correlation between wind speeds and turbidity in CZ and KW implies in-coming, off-site transportation of suspended dust, which was also observed by *Masmoudi et al.* [2003] in their radiometric measurements of the influx of Saharan dust into Tunisia.

The maximum AOD of 0.69 (hour 69) was predicted at CZ for the September 23 to 25, 1999 event (Figure 5), followed by an AOD of 0.4 (hour 56) at KW for the same event (Figure 6) and AOD of 0.3 in CZ (hour 17) for the September 11, 1993 event (Figure 7). These maximum values are comparable to radiometric measurements at λ = 501 nm in Kwangju, South Korea during the Asian dust period, which yielded peak AOD values of 0.71 to 0.76 [*Ogunjobi et al.*, 2004] and AOD values exceeding 0.75 in Dunhuang, China during dust outbreak episodes [*Xiangoa et al.*, 2004]. The lower end of these predictions (AOD of 0.3 in CZ, September 11, 1993) whereas, is comparable to monthly mean averages exceeding 0.3 (λ = 280 to 400 nm) measured by *Zakey et al.* [2004] which was attributed to the influx of fine desert dust during the spring season in Cairo. The predicted AOD values in this study are also within the maximum global seasonal averages (0.4 to 0.5) as predicted by *Tegen and Fung* [1994].

5.3.1 Sensitivity Analyses

The sensitivity of the model parameterizations to size fractionation of the fine and coarse particle size categories and Q_{ext} values at 500 nm was analyzed. The modeled clay to

silt ratio of 48 %: 45 % has a mass median diameter (MMD) of 1.56 μm and perturbations were applied to this ratio by increasing the clay or silt mass while maintaining the overall mass distribution of 93 % from particles in the modeled size range (radius between 0.1 to 3.0 μm). Hence, perturbations resulted in a MMD of 1.42 μm (5 % increase in clay mass contributions), 1.34 μm (10 % increase in clay mass contributions), 1.26 μm (15 % increase in clay mass contributions), 1.7 μm (5 % increase in silt mass contributions), 1.9 μm (10 % increase in silt mass contributions) and 1.98 μm (15 % increase in silt mass contributions). With a MMD of 1.26 μm, there was a 20 to 23 % increase in AOD reflecting higher turbidity due to an increase in fine particles whereas a MMD of 1.98 μm resulted in the largest decrease in AOD (18.5 to 20.5 %).

However, most dust events are expected to be dominated by coarse particles. *Xiangao et al.* [2004] obtained a volume concentration ratio of coarse ($r > 0.6$ μm) to fine ($r < 0.6$ μm) particles of 30 from radiometric measurements during a desert dust storm in China. To consider this aspect, equivalent volume concentrations (based on r_i, ρ and f) were computed for the MMD of 1.98 μm and the ratio of coarse ($r > 1$ μm) to fine ($r < 1$ μm) particles was ~ 37. Therefore, if dust events in eastern Washington were dominated by coarser particles (i.e. higher mass contributions from silt particles), the AOD values modeled in this study would have been overestimated by ~ 20 %. However, soils in this region consist of almost 4 % materials in the PM_{10} size range [*Saxton* 1995], which may result in a lower coarse to fine particle ratio in the windblown dust (i.e. MMD < 1.98 μm). Particle count ratios during windy (7 to 9 m s^{-1}) and non-windy (< 4.5 m s^{-1}) periods in eastern Washington by *Claiborn et al.* [1998] also indicated a ~1.5 to 2.5 factor enhancement in

number concentrations for fine particles in the size categories of 1.35 and 2.05 μm, respectively.

The CRI value determines the optical properties of a particle, in particular Q_{ext}, which was utilized to compute AOD in this study (equation 1). To test the sensitivity of the model parameterizations to variations in Q_{ext} (at 500 nm), several other CRI values utilized for atmospheric dust were also analyzed. These values were 1.55 – 0.004i [*MacKinnon et al.*, 1996], 1.57 – 0.015i [*Torres et al.*, 1998] and 1.52 – 0.008i [*Jennings* 1993]. The CRI value of 1.55 – 0.004i was utilized to infer AOD from satellite retrievals of a dust storm over Owens Lake (California). Comparisons with ground based radiometric measurements yielded an error range of ± 20 to ± 50 %, with respect to the inferred AOD values [*MacKinnon et al.*, 1996]. *Torres et al.* [1998] utilized 1.57 – 0.015i to represent the composition of Saharan dust in their study to characterize aerosols from space. *Jennings* [1993] utilized 1.52 – 0.008i to represent arid dust, comparable to the modeled CRI value of 1.53 – 0.0078i.

All three CRI values yielded higher AOD values for both events compared to the base case CRI value of 1.53 – 0.0078i. However the magnitude of variations from the modeled value of 1.53 – 0.0078i were < 0.4 % for the CRI value of 1.52 – 0.008i, between 1.5 to 2.0 % for 1.55 – 0.004i and between 6.5 to 10.0 % for 1.57 – 0.015i. Based on these limited analyses, it is hard to ascertain the influence of the real and imaginary part of the CRI on the predicted AOD. However, a positive difference of 2.6 % and 92 % in the real and imaginary parts, respectively, between 1.57 – 0.015i and 1.53 – 0.0078i resulted in the highest variations in AOD predictions (6.5 to 10.0 %). The absorptive nature of mineral dust, as reflected in the imaginary part of the index, is considered critical in assessing its climatic

impact, however, the lack of information on dust mineralogy and composition hinders an accurate estimate of the CRI for dust from various source regions [*Tegen* 2003, *Sokolik and Golitsyn*, 1993].

The overall results from the sensitivity analyses indicate that uncertainties in the optical properties of the mineral dust may result in a 10 % overestimation of the AOD values. This is less than the potential 20 % overestimation due to uncertainties in the size fractionation of mineral dust. Therefore, a reasonable estimate of the potential error margin in the predicted AOD values for all events is ± 10 to ± 30 %. However, this estimate does not include the overall uncertainties in the predicted PM_{10} concentrations arising from variability in the predicted meteorology and / or parameterization of the dust emission factors for both dust storm events.

5.4 SUMMARY AND CONCLUSIONS

Turbidity parameters were predicted for two regional dust episodes, which occurred on September 11, 1993 and September 23 to 25, 1999 in eastern Washington. Aerosol optical depths (AOD) and Angstrom turbidity parameters (β) were predicted over a λ range of 400 to 600 nm, utilizing an integrated numerical modeling system that included the MM5 meteorological model, a windblown dust PM_{10} emissions model and the Eulerian CALGRID transport and dispersion model. Due to the lack of corresponding radiometric measurements for validations, temporal variations in β were compared to observed and predicted PM_{10} concentrations at CZ (September 11, 1993 and September 23 to 25, 1999) and KW (September 23 to 25, 1999). There were reasonable agreements between predicted β and observed PM_{10} concentrations, with correlation coefficients ranging from 0.5 to 0.8.

The predicted AOD time series were analyzed with respect to wind speeds and wind directions and at each location, maximum values ranged from 0.3 to 0.7, in good agreement with published maxima in other areas during regional dust storms. Sensitivity analyses were also conducted with respect to size fractionation of fine and coarse particles and optical properties of the dust. The overall results indicated a potential margin of error of 20 % due to a 15 % increase of either fine or coarse particles. Three different complex refractive indexes were utilized to vary extinction coefficients, an important optical property of mineral dust. The maximum overall variation was 10 % due to an increase (with respect to the modeled value) of 2.5 % and 92 % in the scattering and absorptive properties respectively, of the index.

The approach utilized in this study allows reasonably accurate characterization of the temporal variations in optical depths at impacted downwind populated areas during large regional dust storms. However, the results are constrained by the lack of ground based radiometric measurements of atmospheric turbidity during these events that would have provided the best possible method to validate the predictions. While the possibility of utilizing remote sensing products as validation tools is attractive, recent analyses [*Chylek et al.*, 2003] has suggested that current operational satellites based on AOD retrievals at large scattering angles can lead to significant errors in the accuracy of the retrieved products. The results from the indirect approach utilized in this current study to validate the robustness of the model suggest that the assumptions of size classifications, mass distributions and optical properties of windblown dust are reasonable preliminary estimates.

In general, even though improvements are required in the parameterizations of particle sizes and mineralogical compositions to improve the overall accuracy, the predicted

magnitudes suggest that transported dust from agricultural sources in eastern Washington result in turbidity conditions comparable to desert dust. Previous studies [*Sundram et al.*, 2001] have also indicated that the average regional dust storm in eastern Washington may contribute up to 1 % of the global daily average dust flux. This has interesting implications for general circulation models, which are currently designed to reproduce only large scale and seasonal dust patterns, such as the Saharan and Asian dust transport [*Tegen* 2003]. However, large spatial heterogeneities in the transported dust plume and in the vicinity of the source regions of agricultural windblown dust need to be resolved prior to more stringent comparisons. Utilizing these high-resolution models also allows for better characterization of the radiative properties of mineral dust from individual dust events, which has important implications for studies investigating regional atmospheric circulation effects and hence, regional climate variability from these dust storms.

ACKNOWLEDGEMENTS

This work has been supported by the USDA ARS Columbia Plateau (CP^3) PM_{10} project. The authors would like to express their gratitude to all the members of the CP^3 project for their invaluable assistance and advice.

(Tables and Figures follow references)

REFERENCES

Adeyefa, Z. D., and B. Holmgren, Spectral solar irradiance before and during a Harmattan dust spell, *Solar Energy*, *57 (3)*, 195 – 203, 1996.

Cachorro, V. E., R. Vergaz, and A. M. de Frutos, A quantitative comparison of α-Å turbidity parameter retrieved in different spectral ranges based on spectroradiometer solar radiation measurements, *Atmos. Environ.*, *35*, 5117 – 5124, 2001.

Chin, M., P. Ginoux, S. Kinne, O. Torres, B. N. Holben, B. N. Duncan, R. V. Martin, J. A. Logan, A. Higurashi, and T. Nakajima, Tropospheric aerosol optical thickness from the GOCART model and comparisons with satellite and sun photometer measurements, *J. Atmos. Sci.*, *59*, 461 – 483, 2002.

Chylek, P., B. Henderson, and M. Mishchenko. Aerosol radiative forcing and the accuracy of satellite aerosol optical depth retrieval, *J. Geophys. Res.*, 108, 4764, doi: 10.1029/2003JD004044, 2003.

Claiborn, C., B. Lamb, A. Miller, J. Beseda, B. Clode, J. Vaughan, L. Kang, and C. Newvine, Regional measurements and modeling of windblown agricultural dust: The Columbia Plateau PM_{10} program, *J. Geophys. Res.*, *103*, 19753 – 19767, 1998.

Esposito, F., L. Leone, G. Pavese, R. Restieri, and C. Serio, Seasonal variation of aerosols properties in South Italy: a study on aerosol optical depths, Angström turbidity parameters and aerosol size distributions, *Atmos. Environ.*, *38*, 1605 – 1614, 2004.

Ginoux, P., M. Chin, I. Tegen, J. M. Prospero, B. Holben, O. Dubovik, and S.-J. Lin, Sources and distributions of dust aerosols simulated with the GOCART model, *J. Geophys. Res.*, *106*, 20255 – 20273, 2001.

Jennings, S. G., *Aerosol effects on climate,* Tucson, University of Arizona Press, Pg. 41, 1993.

Martinez-Lozano, J. A., M. P. Utrillas, F. Tena, and V. E. Cachorro, The parameterizations of the atmospheric aerosol optical depth using the Ångstrom power law, *Solar Energy*, *63 (5)*, 303 – 311, 1998.

Masmoudi, M., M. Chaabane, K. Medhioub, and F. Elleuch, Variability of aerosol optical thickness and atmospheric turbidity in Tunisia, *Atmos. Res.*, *66*, 175 – 188, 2003.

MacKinnon, D. J., P. S. Chavez Jr., R. S. Fraser, T. C. Niemeyer, and D. A. Gillette, Calibration of GOES-VISSR, visible-band satellite data and its applications to the analysis of a dust storm at Owens Lake, California, *Geomorphology*, *17*, 229 – 248, 1996

Niemeyer, T. C., D. A. Gillette, J. J. Deluisi, Y. J. Kim, W. F. Niemeyer, T. Ley, T. E. Gill, and D. Ono, Optical depth, size distribution and flux from dust from Owens lake, California, *Earth Surf. Process. Landforms*, *24*, 463 – 479, 1999.

Ogunjobi, K. O., Z. He, K. W. Kim, and Y. J. Kim, Aerosol optical depth during episodes of Asian dust storms and biomass burning at Kwangju, South Korea, *Atmos. Environ.*, *38*, 1313 – 1323, 2004.

Saxton, K.E., Wind erosion and its impact on off-site air quality in the Columbia Plateau – An integrated research plan, *Transac. of the ASAE, 38*, 1031 – 1038, 1995.

Sokolik, I., and G. Golitsyn, Investigation of optical and radiative properties of atmospheric dust aerosols, *Atmos. Environ.*, 27*A*, 2509 – 2517, 1993.

Sundram, I., C. Claiborn, T. Strand, B. Lamb, D. Chandler, and K. Saxton, Numerical modeling of regional windblown dust in the Pacific Northwest with improved meteorology and dust emission models, accepted for publication in *Journal of Geophysical Research*, 2004, copyright 2004 American Geophysical Union.

Tegen, I., Modeling the mineral dust aerosol cycle in the climate system, *Quaternary Science Reviews*, *22*, 1821 – 1834, 2003.

Tegen, I., and A. A. Lacis, Modeling of particle size distribution and its influence on the radiative properties of mineral dust aerosol, *J. Geophys. Res.*, *101*, 19237 – 19244, 1996

Tegen, I., and I. Fung, Modeling of mineral dust in the atmosphere: Sources, transport and optical thickness, *J. Geophys. Res.*, *99*, 22897 – 22914, 1994.

Torres, O., P. Bhartia, J. R. Herman, Z. Ahmad, and J. Gleason, Derivation of aerosol properties from satellite measurements of backscattered ultraviolet radiation: theoretical basis, *J. Geophys. Res.*, *103*, 17099 – 17110, 1998.

Von Hoyningen-Huebe, W., K. Wenzel, and S. Schienbein, Radiative properties of desert dust and its effect on radiative balance, *J. Aerosol Sci.*, *30 (4)*, 489 – 502, 1999.

Xiangao, X., C. Hongbin, and W. Pucai, Aerosol properties in a Chinese semiarid region, *Atmos. Environ.*, *38*, 4571 – 4581, 2004.

Zakey, A. S., M. M. Abdelwahab, and P. A. Makar, Atmospheric turbidity over Egypt, *Atmos. Environ.*, *38*, 1579 – 1591, 2004.

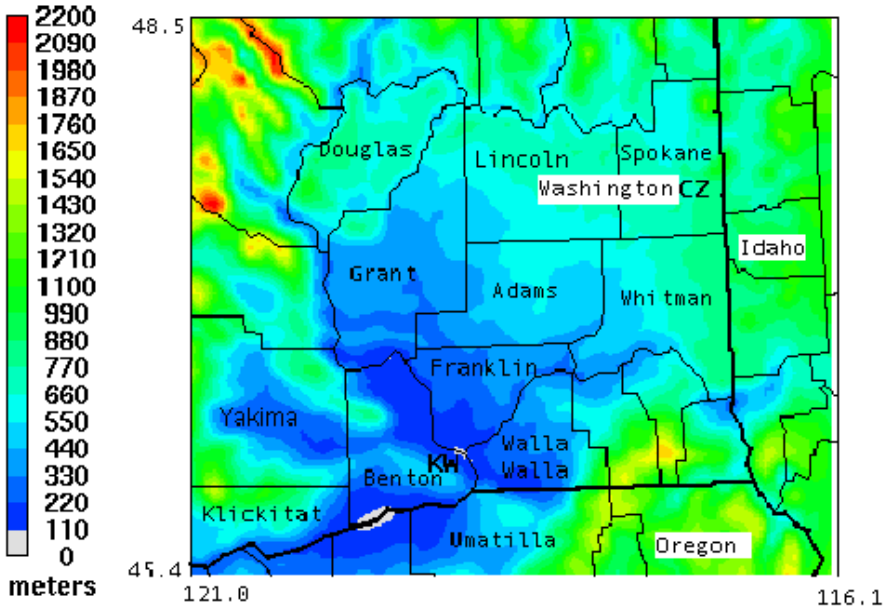

Figure 1. Map of counties in eastern Washington and locations of PM_{10} monitoring sites: Crown Zellerbach (CZ) and Kennewick (KW)

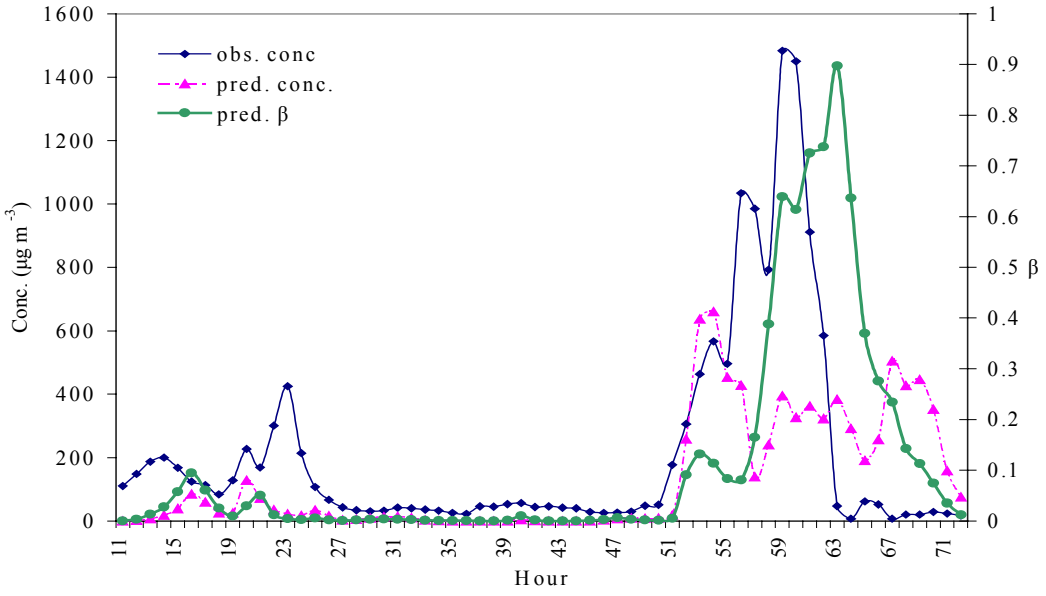

Figure 2. Temporal variations of β, observed and predicted PM_{10} concentrations at Crown Zellerbach (CZ), September 23 to 25, 1999

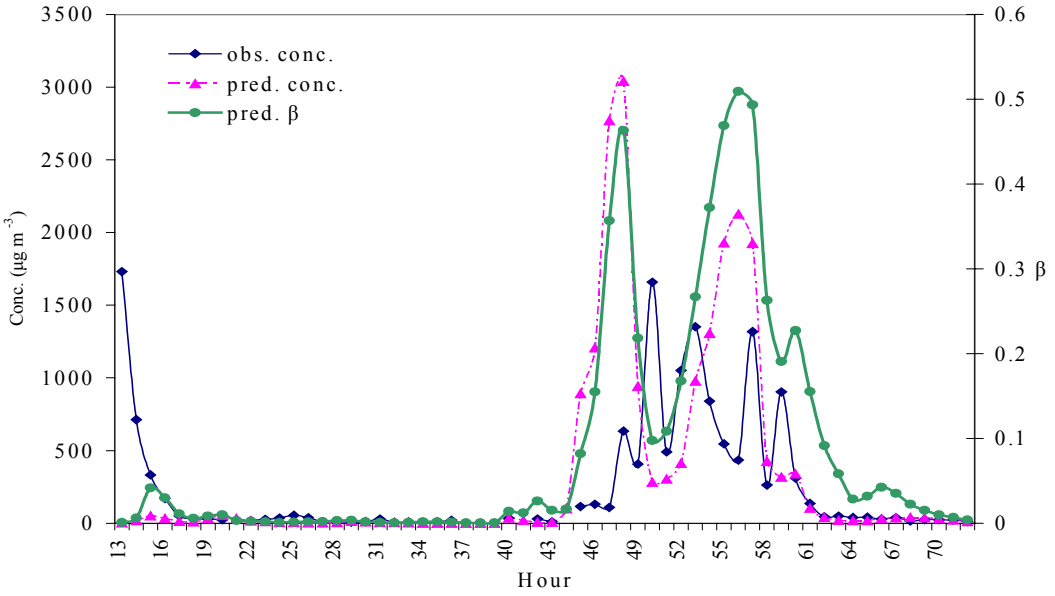

Figure 3. Temporal variations of β, observed and predicted PM_{10} concentrations at Kennewick (KW), September 23 to 25, 1999

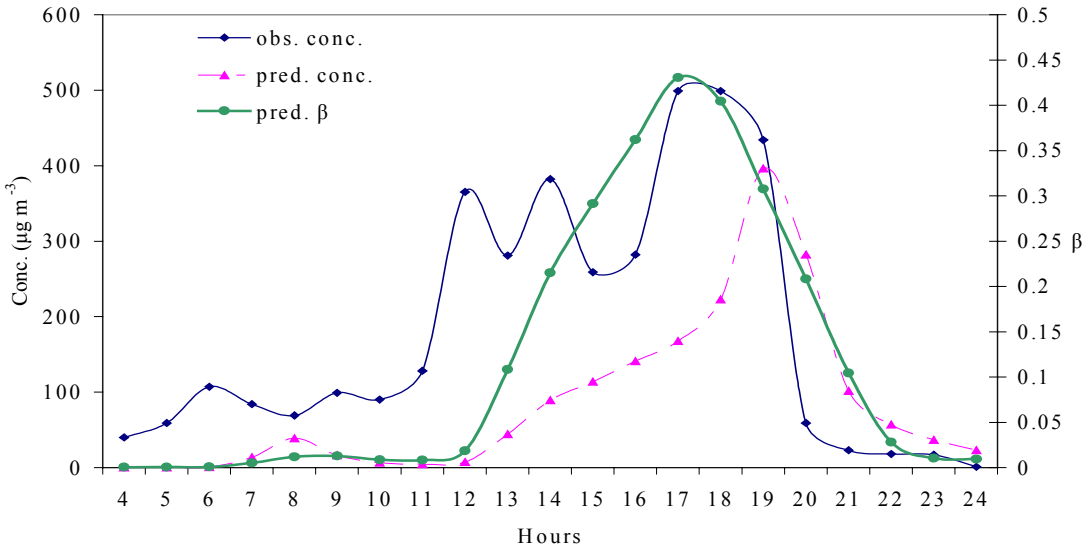

Figure 4. Temporal variations of β, observed and predicted PM_{10} concentrations at Crown Zellerbach (CZ), September 11, 1993

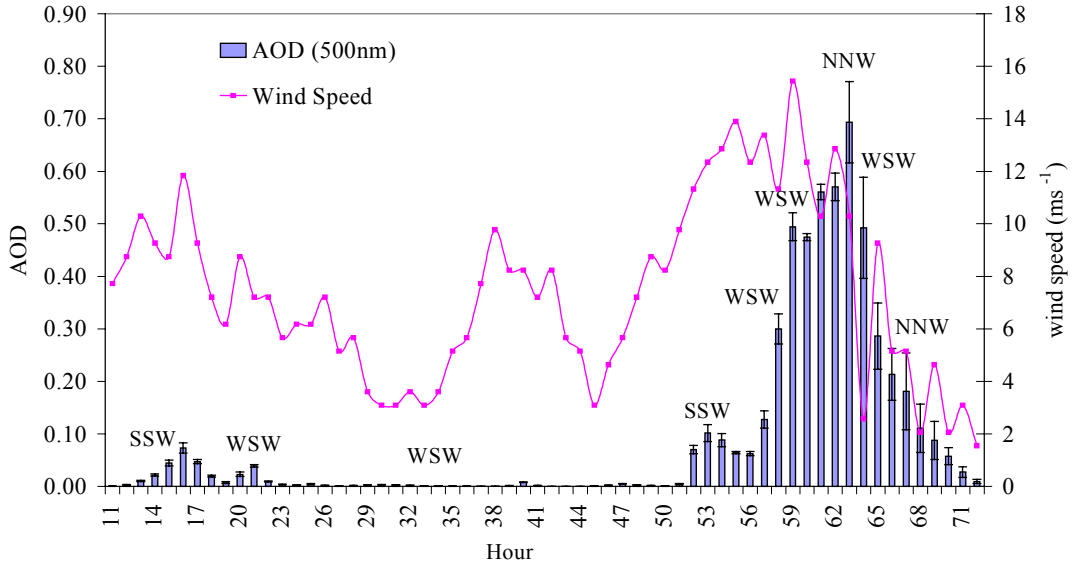

Figure 5. Relationships between AOD, wind speeds and wind directions at Crown Zellerbach (CZ), September 23 to 25, 1999

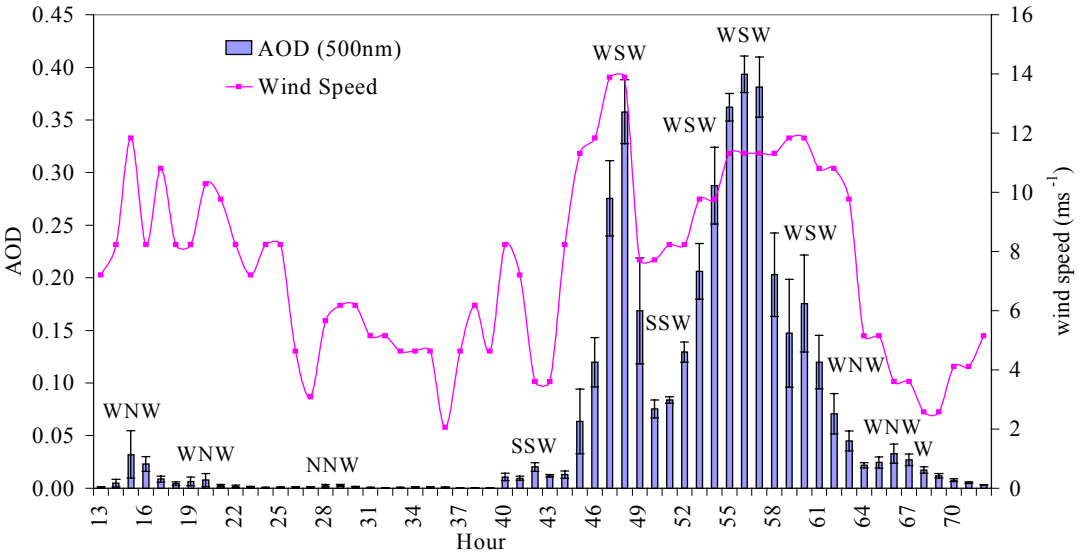

Figure 6. Relationships between AOD, wind speeds and wind directions at Kennewick (KW), September 23 to 25, 1999

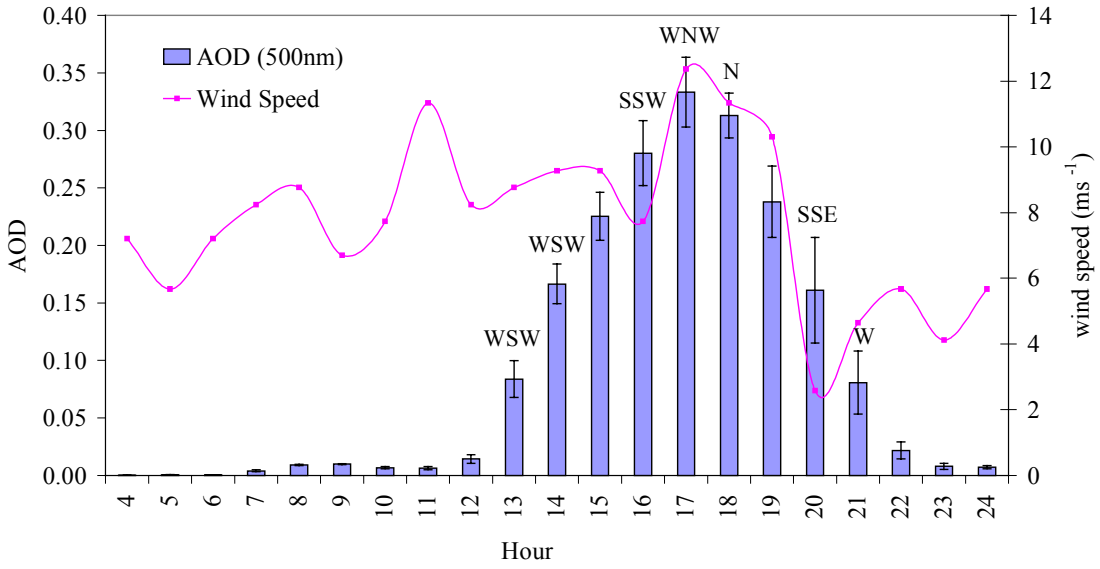

Figure 7. Relationships between AOD, wind speeds and wind directions at Crown Zellerbach (CZ), September 11, 1993

CHAPTER 6: SUMMARY AND CONCLUSIONS

The preceding chapters underscore several important aspects of windblown dust research that encompass the comprehensive objective to assess the physical and radiative properties of the suspended fraction of atmospheric dust, specifically PM_{10}. The most intuitive approach to quantify emissions and concentrations of PM_{10} during a dust storm event is to place dust sampling instruments in strategic locations around potential source regions. This approach has enjoyed considerable success under the Columbia Plateau PM_{10} Project (CP^3). However, we have demonstrated through wind tunnel experiments that the collection efficiencies of some these instruments, in particular the Shrouded Probe (S.P.), Air Quality 10 (AQ-10) and Big Spring Number Eight (BSNE) are within a 40 to 100 % range in conditions akin to a dust storm event; i.e. high wind speeds and dust loading. These results imply that considerable attention should be assigned to data interpretation from field campaigns as measured concentrations could potentially be underestimated by as much as 50 %.

However, there are several aspects that should be addressed in future studies to allow for more stringent evaluations. For consistency, the isokinetic sampler employed should be validated through comparisons with commercially available isokinetic samplers, which can be easily modified for wind speeds < 5 m s^{-1} [*Goossens and Offer*, 2000]. In addition to wind tunnel experiments, the samplers should also be field calibrated to allow improved resolution of potentially larger variations in the dust flow due to unsteady boundary layer winds. Field calibrations would also highlight the effects of gusty winds, which may cause significant temporal variations in the dust transport.

Field measurements of PM_{10} concentrations are critical in any undertaking aimed at characterizing a dust storm event. However, greater resolution of spatial and temporal inhomogeneities of the dust plume can only be achieved by way of numerical models that allow for greater representation of the geographical area. In this regard, we have been successful in developing a modeling system that is capable of identifying sources of PM_{10} emissions and predicting subsequent transport and PM_{10} concentrations in eastern Washington. This modeling system has been validated through direct comparisons of the ratio of predicted to measured PM_{10} concentrations at analogous locations in the region for six dust storm events. Comparison of observed and simulated PM_{10} concentrations for the few available monitoring sites showed that the modeling system yielded good results for the strongest storms, but relatively poor results for the weakest storms. The ratio of observed to predicted concentrations varied from 0.9 for the largest storm to 6.0 for the weakest storm. The good level of agreement obtained for the larger storms did not require the use of a 'dust calibration constant' as has been the case in previous regional modeling studies. A major limitation in the analysis of model performance was the lack of a dense network of PM_{10} sampling stations in the region during these events. For improved corroboration, accessible satellite data should be incorporated into this process and indeed, despite the technical difficulties of interpreting quantifiable data from satellite imagery, this approach has been utilized successfully in regional scaled experiments [*Niemeyer et al*., 1999] and global based circulation models [*Ginoux et al*., 2001].

Besides PM_{10} measurements from sampling stations, we performed sensitivity analyses to authenticate the robustness of our regional modeling system, specifically the PM_{10} emissions model, EMIT-PM. The PM_{10} emissions model was constructed from

statistical relationships among variables that have a significant influence on soil mobilization and subsequently, dust emissions. *Saxton et al.* [2000] and *Chandler et al.* [2002] established these relationships through field campaigns, wind tunnel and laboratory experiments. The sensitivity analyses highlighted the importance of parameters such as threshold wind speeds, random soil roughness, vegetative surface cover and soil crusting in mitigating the effects of wind erosion, especially on dry, fallow lands. Uncertainties in the characterization of some of these parameters, for example, threshold wind speeds and random soil roughness, led to large variations in the predicted PM_{10} emissions, from 39 to 50 Gg. Even though EMIT-PM was developed as a function of the landuse categories and soil classification for eastern Washington, these emission parameters are expected to be useful in most arid or semiarid regions that practice dry land agriculture.

The development of this numerical modeling system also allowed for various simulations characterizing modifications to agricultural practices that could lead to reduction in downwind PM_{10} concentrations. In this study, these modifications encompassed increasing vegetative surface cover and decreasing the coverage of dry fallow lands through conversion to dry crop lands. Both these approaches led to reductions in downwind PM_{10} concentrations; however increasing crop coverage resulted in substantial downwind PM_{10} reductions (> 100 %) while increasing the amount of vegetative cover on existing cropland led to 7 to 9 % reduction in downwind PM_{10} concentrations.

While the predicted PM_{10} emissions and concentrations are subject to uncertainties inherent in the overall modeling system, numerical modeling can be viewed as a beneficial tool for the agricultural community. Even though PM_{10} is regulated under the National Ambient Air Quality Standard, the existing data and models were not specifically designed

for identifying control strategies related to PM_{10} emissions and concentrations [*Saxton et al.*, 1995]. The numerical modeling system developed in this study allows for explicit quantifications of PM_{10} emissions from the various landuse categories common to agricultural practices in eastern Washington, identifies the potential for transported PM_{10} concentrations to impact downwind populated locations and characterizes the potential erosion control strategies that could be implemented to reduce PM_{10} concentrations in downwind locations. From the results of this study, we have identified dry fallow lands as the largest contributor to PM_{10} emissions in eastern Washington, where on average, emissions can exceed 20 Gg per dust storm event. Since soil nutrients are associated with the finer material, this also poses a significant loss of fertile soil for the farmer. We have also been able to identify potential PM_{10} source locations (e.g. Benton, Douglas and Umatilla counties) for each of the six dust storm events simulated in this study and predict the high PM_{10} concentrations (> 200 $\mu g\ m^{-3}$) in locations such as Kennewick and Spokane. In relation to that, potential control strategies that could be implemented by the farming community, which would reduce the PM_{10} concentrations in these locations, were also identified. Since dry fallow lands appear to be the most erosive, converting more of these lands into dry cropping lands would result in immediate reductions of PM_{10} emissions and concentrations downwind during a dust storm event. However, wind erosion could also be controlled through the increase of vegetative surface cover, especially on dry fallow lands.

Resolving atmospheric turbidity from suspended dust is crucial to the primarily study of the radiative and climatic effects of atmospheric dust. We broadened the initial scope of our numerical model to include computations of aerosol optical depths (AOD), a primary indicator of atmospheric turbidity and evaluated the temporal variation of this parameter for

two dust storm events that occurred in eastern Washington. The predictions were evaluated indirectly by assessing the conformance of the predicted Angstrom's coefficient with hourly averaged PM_{10} concentrations measured at several urban locations. There was good temporal agreement between these two parameters with correlation coefficients ranging from 0.5 to 0.8. The predicted maximum AOD values ranged from 0.3 to 0.7, comparable to maximum observed turbidity levels of 0.71 to 0.75 during dust outbreaks in South Korea and China [*Ogunjobi et al.*, 2004, *Xiangoa et al.*, 2004].

Ideally, the AOD predictions should have been validated with ground based radiometric measurements; however, the lack of any spatially and temporally correlated measurements precluded these comparisons. These preliminary estimates however, appear to suggest that windblown dust from agricultural regions may results in turbidity conditions comparable to desert dust storm events which, have been observed to exceed 0.3 [*Zakey et al.*, 2004]. Compared to desert dust storms that last up to 1 week, these windblown dust events tend to last between 24 to 72 hours, however they do occur frequently and with high intensity, and thus may have a significant contribution to the global mineral dust loading. On a regional basis, future studies should investigate the radiative impact of these windblown dust and modifications, if any, to the local and regional atmospheric circulations patterns.

REFERENCES

Chandler, D. G., K. E. Saxton, J. Kjelgaard, and A. J. Busacca, A technique to measure fine-dust emission potentials during wind erosion, *J. Soil Sci. Soc. Am.*, *66*, 1127 – 1133, 2002.

Ginoux, P., M. Chin, I. Tegen, J. M. Prospero, B. Holben, O. Dubovik, and S.-J. Lin, Sources and distributions of dust aerosols simulated with the GOCART model, *J. Geophys. Res.*, *106*, 20255 – 20273, 2001

Goosens, D., and Z. Y. Offer, Wind tunnel and field calibration of six Aeolian dust samplers, *Atmos. Environ.*, *34*, 1043 – 1057, 2000.

Niemeyer, T. C., D. A. Gillette, J. J. Deluisi, Y. J. Kim, W. F. Niemeyer, T. Ley, T. E. Gill, and D. Ono, Optical depth, size distribution and flux from dust from Owens lake, California, *Earth Surf. Process. Landforms*, *24*, 463 – 479, 1999.

Ogunjobi, K. O., Z. He, K. W. Kim, and Y. J. Kim, Aerosol optical depth during episodes of Asian dust storms and biomass burning at Kwangju, South Korea, *Atmos. Environ.*, *38*, 1313 – 1323, 2004.

Saxton, K. E., Wind erosion and its impact on off-site air quality in the Columbia Plateau – An integrated research plan, *Transac. of the ASAE*, *38*, 1031 – 1038, 1995.

Saxton, K. E., D. Chandler, L. Stetler, B. Lamb, C. Claiborn, and B.-H. Lee, Wind erosion and fugitive dust fluxes on agricultural lands in the Pacific Northwest, *Transac. of the ASAE*, *43*, 623 - 630, 2000.

Xiangao, X., C. Hongbin, and W. Pucai, Aerosol properties in a Chinese semiarid region, *Atmos. Environ.*, *38*, 4571 – 4581, 2004.

Zakey, A. S., M. M. Abdelwahab, and P. A. Makar, Atmospheric turbidity over Egypt, *Atmos. Environ.*, *38*, 1579 – 1591, 2004.